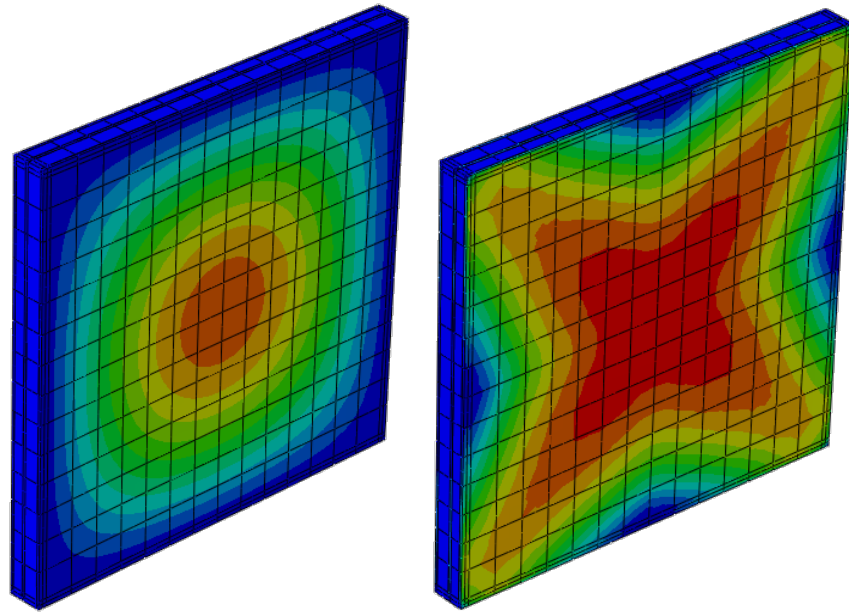# BULGING OF INSULATING GLASS UNITS - Numerical and Experimental Analysis

MARTIN ANDERSSON and SIMON NILSSON

Master's Dissertation

BULGING OF INSULATING GLASS UNITS

Numerical and Experimental Analysis

MARTIN ANDERSSON and SIMON NILSSON

Preface

This master's dissertation was carried out at The Division of Structural Mechanics at the Faculty of Engineering, Lund University. The work started in January 2014 and was finished in June 2014.

We would like to express our gratitude to our supervisor Ph.D. Kent Persson for always taking time for us and for sharing his knowledge concerning the finite element modelling. Special thanks to Ph.D. student Johan Stein for help concerning the experimental analyses.

We would also like to thank Anders Hjalmarsson and Sven Ängbom, Inwido for making it possible to manufacture the insulating glass units.

Finally we would like to thank our families and friends for the support during our education. Special thanks to Fredrik Jönsson for proofreading this report.

Lund, June 2014

Martin Andersson and Simon Nilsson

Abstract

Insulating glass unit (IGU) is separated double or triple glass panes with closed cavities in between, usually filled with argon to reduce the heat transfer. When a construction like this is exposed to temperature variations the volume of the gas will change and pressure changes will occur. The glass panes will bulge which will give displacements and stresses in the glass panes. For large dimensions of the insulating glass along with large temperature variations give a high bulge of the glass panes but the stresses are relatively small. For small dimensions the bulging of the glass panes are smaller but the stresses can be so high that the glass must be toughened. The change of atmospheric pressure can also increase the bulging of the glass panes.

There is a demand for integrated blind in insulating glass. An integrated blind will not be in the way and it would ease the cleaning but during a cold day the integrated blind may be clamped between the glass panes due to the bulging. During an extremely cold day or a warm and sunny day the stresses in the glass panes can instead be so high that the glass may crack. There are many parameters affecting the bulging of the insulating glass e.g. the geometry, glass type and the magnitude of the load. These parameters were investigated in this thesis using modelling analyses and experimental analyses.

The temperature variation through the IGU was formulated with a 1D-FE model in the middle of the IGU. The average temperatures in the cavities were calculated and used in a finite element model made in Abaqus/CAE where the IGU was modeled. The difference from the initial temperatures and the temperatures in the cavities when the IGU was installed gave the pressure change calculated with the ideal gas law. The difference between the initial pressure in the cavities and the atmospheric pressure were used as an external load. The finite element model was used to determine the stresses and the displacements of the glass panes. The 1D-FE model and the finite element model were verified with experimental analyses in a climate chamber (Hotbox).

The temperature in the middle glass was approximately 1-2°C higher than the calculated temperature with the 1D-FE model, which is due to the heat transfer change as an effect of the bulging. When the IG units was exposed to cold temperature a remaining bulging occurred in glass panes of 1-4 mm on each side of the IG units. The total bulging of the finite element model was approximately 1 mm to high than the experimental tests neglecting the remaining bulging.

A parameter study was made changing parameters such as the geometry of the IGU, glass type and magnitude of the load. The choice of gas did not have a major effect on the bulging of the glass panes but it did have a big influence on the insulating capacity. The thickness of the glass panes was found out to have a big effect on the bulging. When the thickness of one glass pane was increased the bulging of that glass pane decreased but the bulging of the other two glass panes increased.

A regression model was carried out to fit a function to the modelled data which makes it possible to change the affecting parameters as the user wants.

Sammanfattning

Isolerglas består vanligtvis av separata åtskiljda två eller tre glas med slutna kaviteter däremellan, ofta fyllda med argon för bättre isoleringsförmåga. Då en sådan konstruktion utsätts för temperaturförändringar kommer gasen att ändra volym och tryckförändringar uppstår. Glasen kommer då att bukta vilket ger förskjutningar och spänningar i glasen. Vid stora dimensioner på isolerglaset tillsammans med höga temperaturlaster blir buktningen av glasen stora men spänningarna desto mindre. Vid små dimensioner blir buktningen mindre men spänningar kan bli så höga att glaset måste härdas. Detta kan förvärras genom en ändring av lufttrycket som ger ytterligare last på konstruktionen och buktningen kan bli större.

Efterfrågan finns på att ha en integrerad persienn i isolerglaset. En integrerad persienn skulle inte vara i vägen och det skulle underlätta städningen men under en kall dag kan persiennen klämmas fast mellan glasen p.g.a. buktningen. Under en extremt kall dag eller en varm solig dag kan spänningarna i glasen istället bli så höga så att glasen kan spricka. Många parametrar påverkar buktningen av isolerglas t.ex. geometrin, glastyp och lastens storlek. Dessa parametrar undersökt i detta arbete med hjälp av modellering och experimentella tester.

Temperaturvariationen i isolerglas beräknades fram med en 1D-FE modell genom mitten av isolerglaset. De beräknade medeltemperaturerna i kaviteterna användes i en finita element modell gjord i Abaqus/CAE där isolerglaset modellerades. Skillnaden mellan gasens temperatur vid tillverkning och temperaturen då isolerglaset var i bruk gav en tryckförändring som beräknades med den ideella gas lagen. Skillnaden mellan gasens tryck vid tillverkning och lufttrycket gav ytterligare last på isolerglaset. Finita element modellen användes för att bestämma förskjutningarna och spänningarna i glasen. 1D-FE modellen och finita element modellen verifierades med experimentella tester i en klimatkammare (Hotbox).

Temperaturen i mittenglaset visade sig vara ca 1-2 grader högre än den beräknade temperaturen med 1D-FE modellen som beror på att värmeöverföringen ändras som en effekt av buktningen. Efter att isolerglasen hade varit utsatt för temperaturlast i Hotboxen så fanns en kvarstående buktning på 1-4 mm på vardera sida. Den totala buktningen beräknad med finita element modellen visade ca 1 mm högre buktning än vad som mättes upp, detta då man bortsåg från den kvarstående buktningen.

En parameterstudie gjordes där parametrar så som geometrin, glastyp, gastyp och storleken på lasten ändrades. Valet av gas visade sig ha en liten påverkan på buktningen av glasen men desto större påverkan av isolerförmågan. Tjockleken på glasen visade sig ha en stor betydelse på buktningen. När tjockleken på ett glas ökades så minskade buktningen av detta glas men buktningen ökade istället för de två andra glasen.

En regressionsmodell gjordes där en funktion anpassas till erhållen modellerad data vilket gör det möjligt för användaren att själv ändra de parametrar som har studerats.

Notations

IGU	Insulating glass unit	

Constants

g	Gravitational acceleration	9.81 [m/s^2]
σ	Stefan-Boltzmann's constant	5.67·10^{-8} [W/(m^{2}K^4)]
R_c	Gas constant	8.314 [J/(molK)]
I_o	Solar radiation intensity on the Earth surface	1090 [W/m^2]

Symbols

a_n	Absorbance for each glass	[-]
a_{tot1}	Total absorbance of the first/outer glass pane	[-]
a_{tot2}	Total absorbance of the second/middle glass pane	[-]
a_{tot3}	Total absorbance of the third/inner glass pane	[-]
b_{spacer}	Width of spacer	[m]
c_p	Specific heat capacity for gas	[J/(kgK)]
dh_{spacer}	Displacement of spacer	[m]
$f_{b;k}$	Characteristic value of bending strength of prestressed glass	[Pa]
$f_{g;d}$	Design value of strength of annealed/prestressed glass	[Pa]
$f_{g;k}$	Characteristic value of bending strength of annealed glass	[Pa]
h_{cavity}	Heat resistance in cavity ($h_{cc}+h_r$)	[W/K]
h_{cc}	Heat resistance of conduction and convection in cavity	[W/K]
h_{glass}	Heat resistance in glass pane	[W/K]
h_i	Heat resistance on the inside	[W/K]
h_n	Heat resistance in glass pane, cavity or outside/inside	[W/K]
h_o	Heat resistance on the outside	[W/K]
h_r	Heat resistance of radiation in cavity	[W/K]
$h_{r,space}$	Heat resistance coefficient for radiation to outer space	[W/m^{2}K]
h_{spacer}	Height of spacer	[m]
k_{mod}	Factor considering load duration	[-]
k_{sp}	Factor considering the glass surface profile	[-]
k_v	Factor considering the strengthening of pressed glass	[-]
p	Pressure in cavity	[Pa]
q	Heat flux	[W/m^2]
r_n	Reflectance for each surface	[-]

t_{gn}	Thickness for each glass pane	[m]
t_n	Transmittance for each glass	[-]
t_{si}	Distance of inner space	[m]
t_{so}	Distance of outer space	[m]
C_1, C_2 and C_3	Coefficients considering a closed space	[-]
E_{spacer}	Young's modulus of spacer	[Pa]
F_{spacer}	Force on spacer	[N]
I_{eff}	Effective solar intensity	[W/m^2]
L_{spacer}	Length of spacer	[m]
M	Molecular mass of gas	[kg/mol]
Nu	Nusselt number	[-]
Ra	Rayleight number	[-]
R_i	Transfer resistance on the inside	[m^{2}K/W]
R_o	Transfer resistance on the outside	[m^{2}K/W]
T_m	Mean temperature in cavity	[K]
T_n	Temperature in glass pane surface or outside/inside	[K]
T	Temperature difference	[K]
U	Total heat resistance	[W/m^{2}K]
α	Angle of incidence for solar radiation	[°]
α_c	Heat resistance coefficient for convection	[W/m^{2}K]
α_r	Heat resistance coefficient for radiation	[W/m^{2}K]
β	Thermal expansion coefficient, $1/T_m$	[1/K]
$\gamma_{M;A}$	Material partial factor for annealed glass	[-]
$\gamma_{M;V}$	Material factor for surface prestress	[-]
ε_n	Emissivity for each glass pane	[-]
λ_{gas}	Thermal conductivity for gas	[W/(mK)]
λ_{glass}	Thermal conductivity for glass	[W/(mK)]
μ	Dynamic viscosity for gas	[Pa·s]
ρ	Density of gas	[kg/m^3]

Contents

1 Introduction

1.1 Background

Insulating glass (IG) is widely used today to increase the insulating capacity of buildings. An insulating glass unit (IGU) is usually two or three separated glass panes with sealed cavities in between. The cavities are usually filled with argon to reduce the heat transfer. When a construction like this is exposed to temperature variations the volume of the gas will change and the glass panes will bulge, see Figure 1. The change of atmospheric pressure will also affect the bulging of the IG units.

To keep solar radiation out of the building a blind can be used. For insulating glass the blind is usually on the inside of the IGU where it can be in the way for e.g. lamps or flowers. A blind integrated into the IGU have several advantages since it is not in the way and it does not require cleaning.

Problems may occur during a cold day where the integrated blind may be clamped between the glass panes due to the bulging. For extremely low or high temperatures in the IGU, high tensile stresses in the glass may occur and the glass can break. Since glass is more sensitive to tensile stresses due to the micro-cracks in the material, the glass must be toughened if a risk of too high tensile stresses exists.
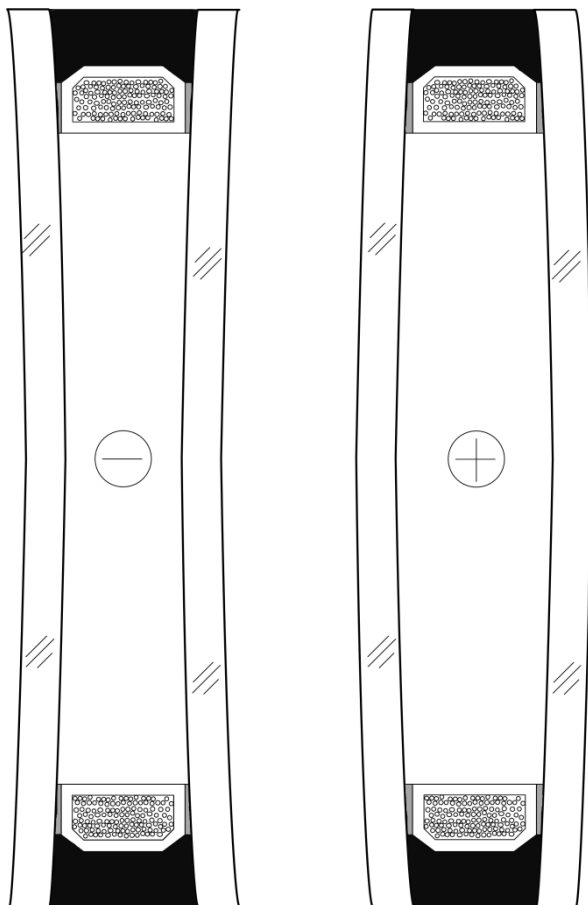

Figure 1. Inwards and outwards bulging of the glass panes.

1.2 Objective and Method

The objective of the study is to analyse the bulging of IG units for varying parameters such as the geometry and the magnitude of the loads. The primary goal is to determine the possibility of having an integrated blind in an IGU and to predict when the stresses become too high and the glass must be toughened.

The temperature through the IGU is in the study determined with a one dimensional model. Static load analysis will be carried out in the finite element program Abaqus/CAE from which the bulging and the stresses are obtained. To verify the temperatures through the IGU and the FE-model, experimental analyses will be carried out in a Hotbox where the temperatures in the various glass panes and the bulging will be measured. A regression model with data from the FE-model was made aiming at making it possible to determine the stresses and the displacements in the glass panes for a specific IGU and load combination.

1.3 Limitation

When calculating the temperatures in the IGU with the one dimensional model is used, the method is not taking into consideration the different heat transfer that occurs at the boundaries of the IGU. When the glass bulge the heat transfer changes due to change in the geometry, an effect that is not taken into consideration in the model.

The material properties of the sealants are varying with the temperature. The sealants in the model are assumed to have a linear elastic behaviour independent of the temperature.

1.4 Outline

- Chapter 2: The components of an IGU and the manufacturing process is described.
- Chapter 3: The heat transfer in an IGU is described and a one dimensional FE model is introduced to calculate the temperature distribution through the IGU. Further, the finite element method, Abaqus/CAE, Python and the implementation of Python is generally described. Furthermore the design strength of glass is calculated with the European standard.
- Chapter 4: Experimental analyses are presented.
- Chapter 5: The FE model is described, a model to calculate the displacement and stresses in the glass panes.
- Chapter 6: A comparison between the FE model and the experimental analyses are carried out and a discussion about the compliance.
- Chapter 7: The parameter study is described i.e. the parameters that were changed and analysed. Some examples of the parameter study are carried out and the results are presented.
- Chapter 8: The regression model is generally described.
- Chapter 9: A discussion of the results is presented.
- Chapter 10: A conclusion of the work and some suggestions of further work are given.

2 Insulating Glass Unit

The basic components of an IGU are two or three panes separated by a spacer to create a cavity between the glass panes. To avoid moisture in the cavity the spacer is filled with desiccant. The cavity is filled with a gas, usually argon to increase the thermal insulating capacity. To keep the gas in the cavity and prevent leakage a sealant with low permeability called primary sealant is placed between the glass panes and the spacer. A secondary sealant is placed between the panes, outside and around the spacer for the main bearing function and to protect the primary sealant. The glass can have a low-emissivity (low-E) coating to increase the insulating capacity [16].
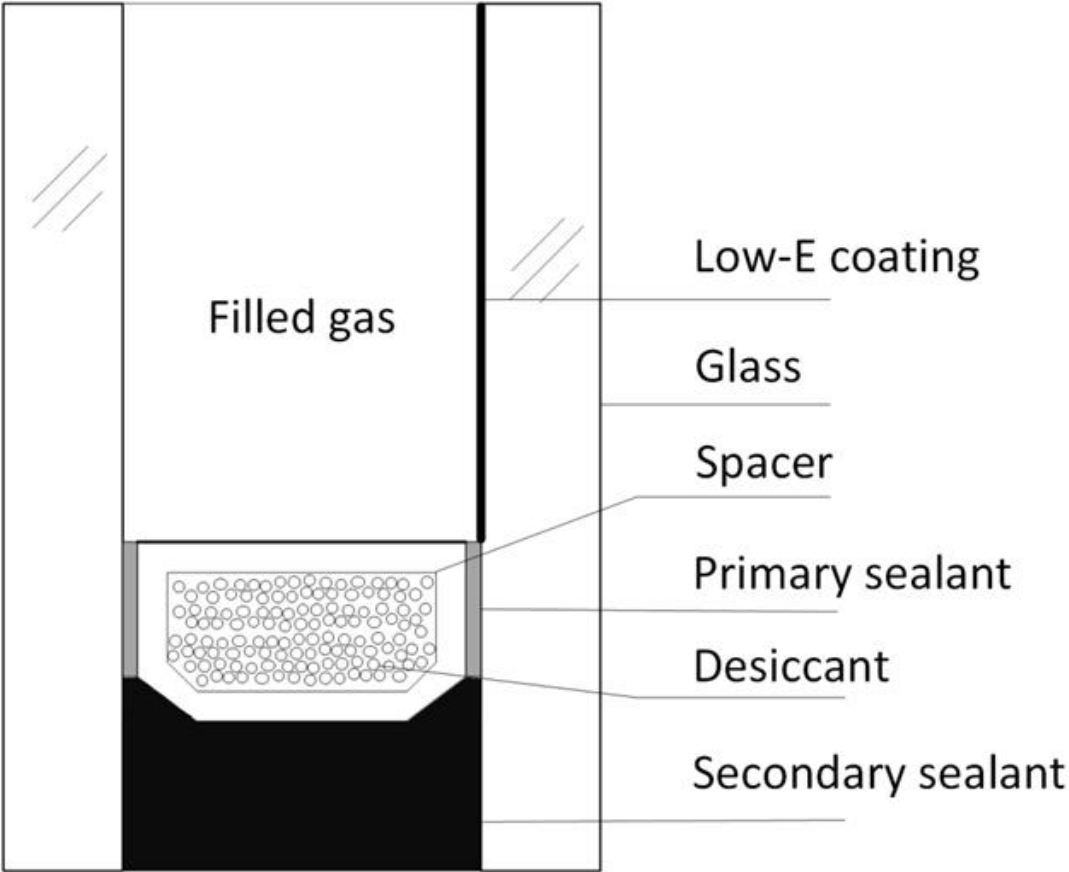
Figure 2. Basic components in an IGU with double sealed system.

2.1 Glass

The constituents of glass are quartz (silicon dioxide), flux and stabilization material. Quartz is the most important constituent of glass; to make good glass the purity of sand is therefore high. The function of the flux is to lower the melting point while the stabilization material increases the resistance against chemicals and moisture. Glass has an amorphous structure meaning that the atoms are arranged in an irregular pattern like liquid which gives the special transparency ability [1]. Glass is a brittle material because of existing micro-cracks in the material which makes glass sensitive to tensile stresses [6].

The material parameters for normal float glass is according to [8], density 2500 kg/m^3, Young's modulus is 70 000 MPa and Poisson's ratio 0.22.

The heat conductivity of glass is 0.81 W/(mK) and the specific heat capacity is 840 J/(kgK) according to [1].

The glass types in an IGU can vary depending on the function of the IGU. Low-emissivity glass is used for a better insulating capacity. Solar control glass is used to prevent solar radiation transmitting through the building. Further, fire protective glass is also used in IGU's to resist a fire during a specific time. Furthermore, safety glass such as laminated and toughened glass is used for special safety cases [11]. In this report the authors will investigate the IGU focused on the insulating capacity i.e. annealed glass and low-E coatings will be used.

2.1.1 Annealed glass

Nowadays the most common way of manufacturing annealed glass is by using the float process. In the float process the raw materials are molten at a temperature of 1550°C. The molten glass is thereafter floating on a plane bed of molten tin which the temperature is lowered to 1100°C. When the molten glass has reached a temperature of 600°C it is slowly cooled down to reduce built in stresses. With the floating process it is easy to control the thickness of the glass. The glass is cut to preferred dimensions or delivered with large dimensions of approximately 6x3 m to be cut later [11].

Manufactured glass has nominal thickness with tolerances according to EN 572-2 [9].

Nominal thickness [mm]	Tolerance [mm]
2, 3, 4, 5, 6	± 0.2
8, 10, 12	± 0.3
15	± 0.5
19, 25	± 1.0

Table 1. Nominal thickness and tolerance of annealed glass [9].

Annealed glass is the basic product of flat glass, used as a primal component for making other products such as toughened glass or low-emissivity glass. When annealed glass breaks, sharp shards with various sizes will appear and the risk of cutting is high. [2]

2.1.2 Toughened glass

Micro-cracks in glass decrease the tensile strength of the material. Glass is toughened to reduce the effects of the micro-cracks. Toughened glass is annealed glass heated up to approximately 600°C followed by a rapid cooling of the surface. When the inner portion is cooling to room temperature compressive stresses emerge at the surface, balanced by tensile stresses at the inner portion. With this process a higher bending- and tensile strength is achieved. The Young's modulus will be unchanged by this process. Toughened glass has a higher resistance to unevenly distributed temperatures than annealed glass due to the built in

stresses. Toughened glass breaks into small and regular granules and the risk of cutting is relatively small [3].

2.1.3 Low-emissivity glass

Infrared transparency is a problem in buildings. In the summer the indoor temperature increases due to the IR radiation through the insulating glass. On the winter a thermal loss from the building occurs through the insulating glass. Low-emissivity or low-E glass is annealed glass glazed with a thin metallic coating on the surface, see Figure 2. A low-E coating is designed to reflect IR radiation. This will reduce the thermal loss in the winter and increase the reflections of solar radiation in the summer. Different properties of the IGU will be obtained depending on the number of and where the low-E coating is placed [6].

There are two types of coatings, soft- and hard coating. Soft coating which is based on silver is delicate and easily damaged, therefore its surface is always placed towards the cavity. Hard coating is tin oxide sprayed on the hot float glass surface which gives, at least, as durable surface as annealed glass and can therefore also be placed on the outside of the glass. A glass with a hard coating could also be toughened with the same process as used for annealed glass [3].

The emissivity factor for a typical low-E glass is 0.037 which describes how much radiation the glass emits to the surroundings compared to a black body. Comparing with annealed glass the low-E glass emits less energy to the surroundings. The emissivity factor for annealed glass is 0.837 [32].

2.1.4 Choice of glass

Both annealed glass and low-E glass will be modelled in this work. Toughened glass is when the stresses become too large in the glass. The material stiffness properties are the same for these types of glass but the optical properties differ for between annealed- and low-E glass.

The nominal thickness of the glass is chosen to be 2, 4, or 6 mm depending on the configuration of the IGU. Taking into consideration that the thickness could vary with the tolerance when manufactured, the glass thickness to be used in the model is shown in Table 2.

Nominal thickness [mm]	Thickness in model [mm]
2	1.8
3	2.8
4	3.8
6	5.8

Table 2. Nominal thickness, thickness to be used in the model.

Perpendicular incoming solar radiation to an ordinary annealed glass surface results in a reflection of the solar radiation by a certain percentage. The remainder will transmit through the glass and absorb in the glass. With an increased thickness the glass will absorb more energy and less will be transmitted, see Table 3.

Thickness [mm]	Transmittance [%]	Reflectance [%]	Absorbance [%]
3	87	8	5
4	85	8	7
6	79	7	14
8	76	7	17

Table 3. Optical properties of annealed glass. [32]

The emissivity factor is lower for low-E glass than for annealed glass and the optical properties changes when a low-E coating is placed on a surface. The reflectance and absorbance is dependent on which side of the glass the incoming solar radiation hits but the transmittance is independent of this. For direct solar radiation on the coated side, the optical properties is shown in Table 4.

Thickness [mm]	Transmittance [%]	Reflectance [%]	Absorbance [%]
3	63	28	9
4	62	28	10
6	59	27	14
8	57	27	16

Table 4. Optical properties of low-E glass when hit directly by solar radiation [32].

For indirect solar radiation on the coated side the optical properties is shown in Table 5.

Thickness [mm]	Transmittance [%]	Reflectance [%]	Absorbance [%]
3	63	26	11
4	62	25	13
6	59	20	21
8	57	18	25

Table 5. Optical properties of low-E glass when hit indirectly by solar radiation [32].

2.2 Spacer

The spacer separates the glass panes in the IGU to form a cavity. Nowadays the most common material of the spacer is stainless steel or a combination of plastic and metal. Since the glass panes are connected at the edges through the spacer and the sealant, a large amount of heat conduction occurs there. Stainless steel is better in reducing the heat conductivity compared to the earlier aluminium spacer, but the plastic/metal combination provides an additional reduction in heat conduction. Metals such as aluminium and stainless steel are gas-impermeable while plastic is not. A stainless steel or aluminium foil is therefore used to make the plastic/metal spacer gas-impermeable [16].

2.2.1 Choice of spacer

Some experimental stress-strain tests were made for the plastic/metal spacer with different height [20]. The spacers had a length of 150 mm and a width of 6 mm. The spacers were placed between two plates and pressed together. The test results are shown in Figure 3 for

some various height of the spacer. The initial stiffness of these spacers was found to be independent of the spacer height.
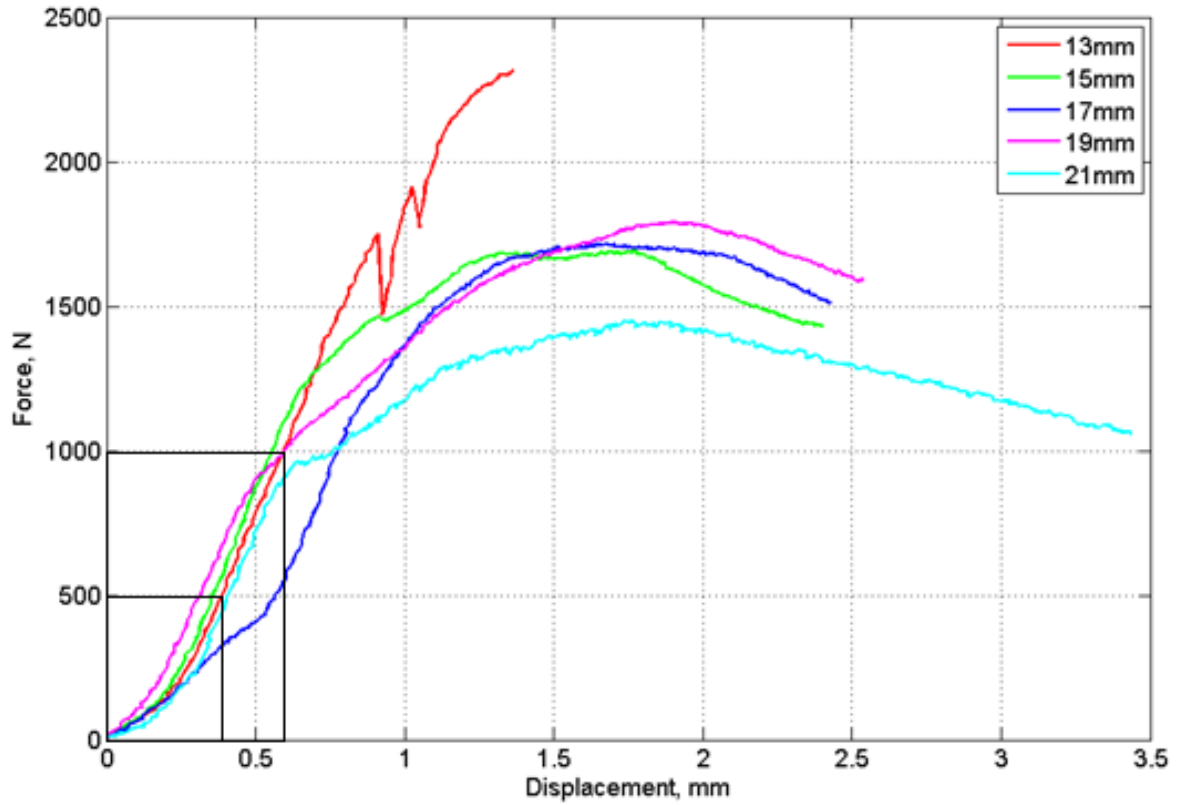
Figure 3. Force-displacement curve of plastic/metal spacer with various heights [20].

The spacer is assumed to have a linear elastic behaviour and the Young's modulus can be calculated with Hooke's law [15].

$$\sigma_{spacer} = E_{spacer}\varepsilon_{spacer} \quad \leftrightarrow \quad E_{spacer} = \frac{\sigma_{spacer}}{\varepsilon_{spacer}} = \frac{F_{spacer} \cdot h_{spacer}}{A_{spacer} \cdot dh_{spacer}} =$$

$$= \frac{F_{spacer} \cdot h_{spacer}}{b_{spacer} \cdot L_{spacer} \cdot dh_{spacer}} \tag{2.1}$$

where

F_{spacer} = force on spacer [N].

h_{spacer} = height of spacer [m].

b_{spacer} = width of spacer, 6 mm.

L_{spacer} = length of spacer, 150 mm.

dh_{spacer} = displacement of spacer [mm].

Two points are taken on the curve in Figure 3 to decide the Young's modulus of the spacer: (1000 N, 0.54 mm) and (500 N, 0.35 mm)

With the above mentioned values inserted in Eq

(2.1) the Young's modulus is obtained:

$$E_{spacer} = \frac{(1000 - 500) \cdot h_{spacer}}{0.006 \cdot 0.15 \cdot (0.54 - 0.35) \cdot 10^{-3}} = 2.9 \cdot h_{spacer} \text{ GPa} \tag{2.2}$$

The plastic/metal spacer consists of two materials but is assumed to be a homogenous material with one Young's modulus. The Poisson's ratio was assumed to be 0.3.

Moisture can be trapped inside the cavity when manufactured or permeate through the sealant when the IGU is in use. Desiccants adsorb the moisture and are placed in the hollow of the spacer, see Figure 2.

2.3 Sealant

The sealing of the IGU is performed with a single- or double- sealed method, see Figure 4. In 2003 85-90% of the manufactured IG units in Europe were with the double-sealed method, single-sealed IG units are more common in North America. It is easier to have a longer lifetime of a double sealed system since each sealant in this system is optimized for a specific function. In a single sealed system the sealant must fulfill several properties and therefore it is harder to make an IGU with good functionality [4].
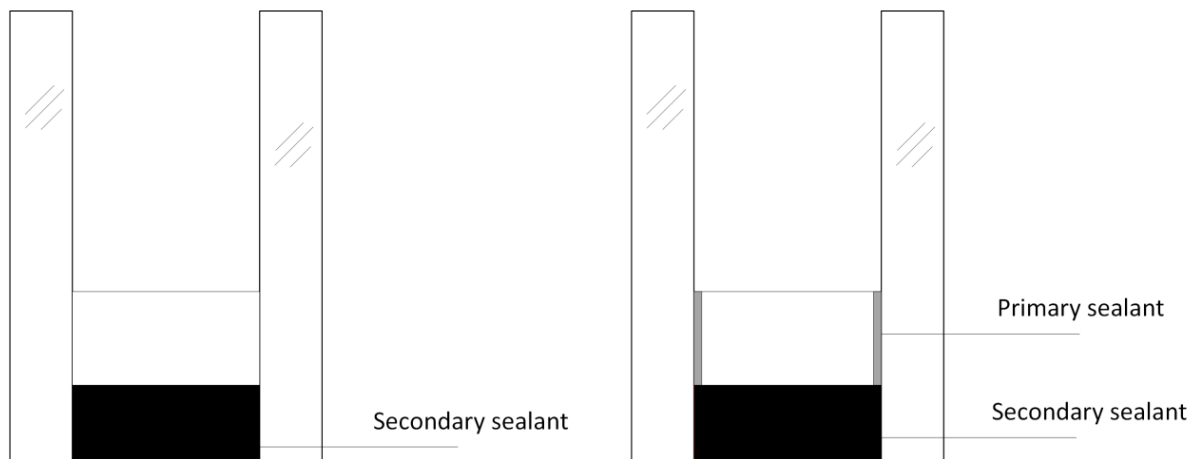
Figure 4. Single sealed system to the left, double sealed system to the right.

In dual-sealed IG units there are two types of sealant. The primary sealant is placed on the edge of the spacer with the function to keep the gas in the cavity and prevent water molecules to permeate through. The secondary sealant is placed in the hollow with the function of protecting the primary sealant and bonds the two glass panes together. The secondary sealant also reduces permeability of gas and water molecules. In a single-sealed system the secondary sealant has to be gas-impermeable and hold the glass panes together [16].

The sealants in the IGU are of major importance for the lifetime of the IGU. During a lifetime of an IGU the sealants must withstand cyclical attacks from its surrounding: physical attacks, chemical attacks and physical-chemical attacks [5].

2.3.1 Primary sealant

The permeability of the IGU system depends to a great extent on the primary sealant since the metal in the spacer is gas-impermeable. The primary sealant has to be a barrier to moisture and to gas-leakage. The most common primary sealant is butyl due to its good properties [16].

Butyl has a high resistance to light and heat ageing and has a low permeability for water vapour and fill gases but the adhesion to glass is very sensitive to water exposure. Butyl is a thermoplastic material, meaning that the strength of the material depends on the temperature [5].

The Young's modulus of butyl is dependent of the temperature and is approximately around 2.13-4.25 MPa [25]. The typical thickness is around 0.2-0.6 mm, but a constant thickness is in this work assumed to be 0.3 mm [4].

Since butyl has a poor adhesion to glass when exposed to water a secondary sealant is required to protect the butyl and ensure that the IGU works properly.

2.3.2 Secondary sealant

The secondary sealant's main purpose is for the durability function of the system but it also protects the primary sealant and decreases the permeability. During the service life of the IGU the system have to resist cyclic attacks from the surroundings, as described in the previous section. The most common secondary sealant is polysulphide or polyurethane due to their good adhesive ability. If the secondary sealant is exposed to solar radiation silicone could be used. Silicone has a better resistance to short wave radiation than both polysulphide and polyurethane, but the adhesive ability is lower and the permeability is higher [16]. A minimum thickness of the secondary sealant is 3 mm to protect the primary sealant from moisture [4].The thickness of the secondary sealant is in this work assumed to be 6 mm.

The Young's modulus of the secondary sealant is temperature dependent as shown in Figure 5 [18].
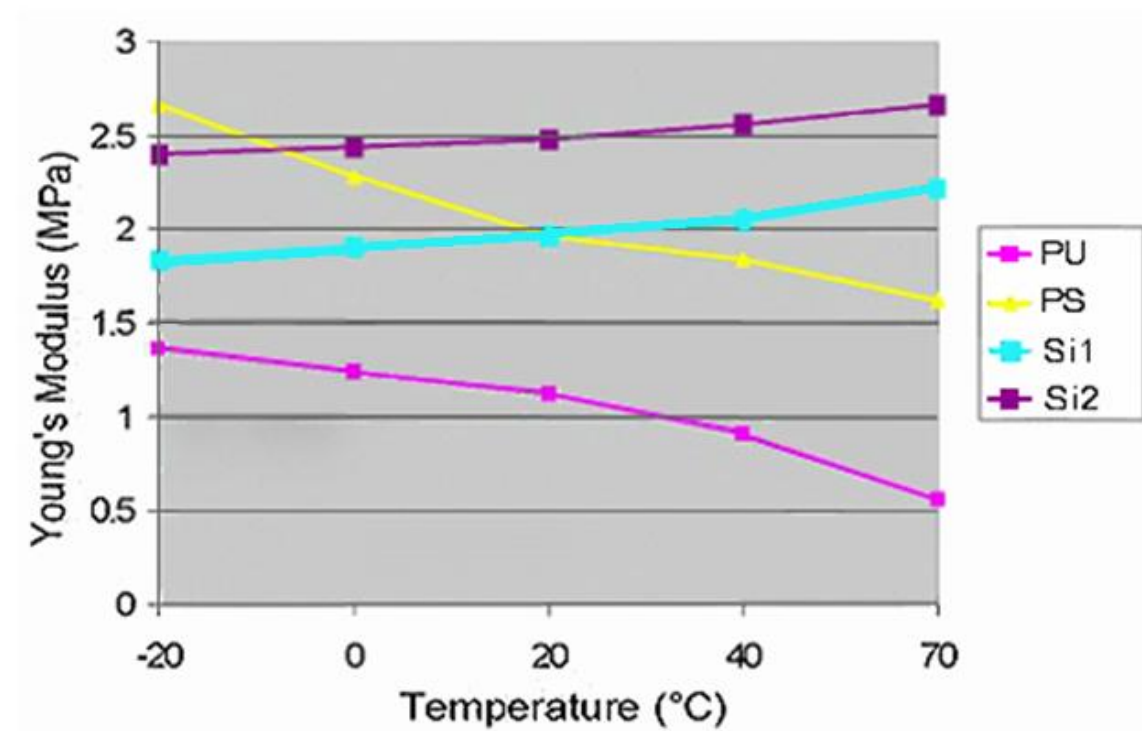

Figure 5. Young's modulus of some secondary sealants as a function of temperature. PU=Polyurethane, PS=Polysulfide and Si=Silicone [18].

The Young's modulus of two types of silicone is shown in Figure 5. The silicone has a typical elastomeric behaviour with the Young's modulus increasing with the temperature. The polysulphide and the polyurethane on the other hand have a decreasing Young's modulus with elevated temperature. These organic sealants have a more thermoplastic behaviour and for elevated temperatures these have the ability to stretch more compared to silicone and the risk for moisture diffusion arise.

Three common types of secondary sealants are polysulphide, polyurethane and silicone which will be described further below.

Polysulphide
Polysulphide is only used in a double sealed system, see Figure 4. Polysulphide is the most common secondary sealant and its properties are well known. Polysulphide has a low permeability for fill gases such as argon and the adhesion to glass is good. The disadvantage of polysulphide is the sensitivity to short wave radiation and the high level of swelling when absorbing water. Both mechanisms result in higher vapour diffusion through the sealant which can affect the primary sealants adhesion to the glass [5].

Polyurethane
Polyurethane is only used in double sealed system as polysulphide. Polyurethane has a good flexibility at low temperatures and has low water vapour permeability. The disadvantage of

polyurethane is the high level of swelling and that it has a higher permeability for the filled gas than polysulphide. Polyurethane is also very sensitive to short wave radiation [5].

Silicone

Silicone can be used in both single- and double sealed systems. It is also known for its good resistance against short wave radiation. In a damp environment silicone absorbs a small amount of water and the swelling is small compared to polysulphide and polyurethane. The disadvantage of silicone is the higher permeability for the filled gas [5].

2.3.3 Choice of sealant

As a primary sealant butyl will be used in the modelling of the IGU's. Polysulphide will be used as a secondary sealant for its good adhesive ability and because it is the most used secondary sealant. 73 % of the double sealed systems in Europe have polysulphide as a secondary sealant [21]. The Poisson's ratios for the both sealants were assumed to be 0.2.

2.4 Cavity

The cavity is filled with air or some noble gas like argon or krypton to improve the thermal insulating capacity. The cavity is filled with a gas content to 90% and the most common gas is argon since krypton is much more expensive [16].

2.4.1 Choice of gas

Table 6 show the linear equation coefficients as a function of temperature. The thermal conductivity, dynamic viscosity and specific heat capacity as a function of temperature are presented for the three gases air, argon and krypton. The molecular mass is presented as well. The values are taken from Table B.1-B.4 [12].

		Air	**Argon**	**Krypton**
Thermal conductivity λ [W/(mK)] $\lambda = a + bT(K)$	a [W/(mK)]	$2.873 \cdot 10^{-3}$	$2.285 \cdot 10^{-3}$	$9.443 \cdot 10^{-4}$
	b [W/(mK^2)]	$7.760 \cdot 10^{-5}$	$5.149 \cdot 10^{-5}$	$2.826 \cdot 10^{-5}$
Dynamic viscosity μ [Pa·s] $\mu = a + bT(K)$	a [Ns/m^2]	$3.723 \cdot 10^{-6}$	$3.379 \cdot 10^{-6}$	$2.213 \cdot 10^{-6}$
	b [Ns/m^{2}K]	$4.940 \cdot 10^{-8}$	$6.451 \cdot 10^{-8}$	$7.777 \cdot 10^{-8}$
Specific heat capacity c$_p$ [J/(kgK)] $c_p = a + bT(K)$	a [J/(kgK)]	1002.737	521.929	248.091
	b [J/(kgK^2)]	$1.232 \cdot 10^{-2}$	0	0
Molecular mass [kg/mol]		$28.970 \cdot 10^{-3}$	$39.948 \cdot 10^{-3}$	$83.80 \cdot 10^{-3}$

Table 6. Properties of three different gases used in IG units [12].

If the cavity is filled with argon or krypton the aim is to have a gas content of 90% [16]. Therefore a linear interpolation of the values in Table 6 will be made with 10% air and 90% filled gas.

2.5   Integrated blind

SL22M is an integrated blind that can be used in an IGU. Possible height is between 300-2500 mm and possible width is between 300-2000 mm. This integrated blind is intended to be used in a cavity with the space distance 22 mm. The bottom rail has a width of 14 mm which will be the decisive width ensuring that the blind will not be clamped when the glass bulge. An assumption is made in this work that if one of the glass panes around the blind bulges more than 3.25 mm, the blind would be clamped. A light colour of the blind is assumed in this work for its low absorption factor and high reflection factor to avoid excessive temperatures in the cavity. S102 is the colour that will be used which has the absorption factor 0.31 and the reflection factor 0.7 [23]. The emissivity of the S102 colour is 0.8 [24].

2.6   Manufacturing

The manufacturing of glass is described in Chapter 2.1. The glass panes are delivered in large dimensions then put on a bench where they are cut into preferred dimensions. If the glass pane has a low-E coating it must be mechanically removed before the cutting to increase protection against corrosion and the bonding strength to the sealant. Different sizes are cut from each glass pane to optimize the glass pane and reduce the waste material, and then placed in order of size. However there is still some waste of the glass which will be recycled.

The spacer is bent to the form of a rectangle and filled with desiccant; the butyl is applied on the edges on both sides of the spacer. The spacer is placed on a glass pane and a second glass pane is placed on the other side. Before the glass panes are pressed together with the spacer the cavity can be filled with a more noble gas than air to a minimum content of 90%. The glass panes are then pressed towards the spacer. The same process is made one more time to obtain a three glass IGU. Finally polysulphide is placed on the outside of the spacer and between the glass panes to hold the IGU together [16].

The study of the bulging will be carried out varying different factors presented below:

- Width: 0.3-1.6 m
- Height/Width ratio: 1-3
- Glass thickness: 1.8, 3.8, 5.8 mm in different combinations in the three glass panes.
- Space distance: 8-27 mm for both inner and outer cavity. 22 mm in the inner cavity when a blind is integrated in the IGU.
- Gas type: air, argon and krypton
- Position and number of low-E coatings: The low-E coatings were usually placed at surface 2 and 5. When a blind was integrated in the IGU some analyses were made with only one low-E coating on surface 2, see Figure 7.

3 Theory

3.1 Heat transfer

The heat transfer through an IGU consists of convection, conduction and radiation [16]. In Figure 6 these are illustrated with a low temperature on the left side and a higher temperature on the right side which gives a heat flow from right to left.
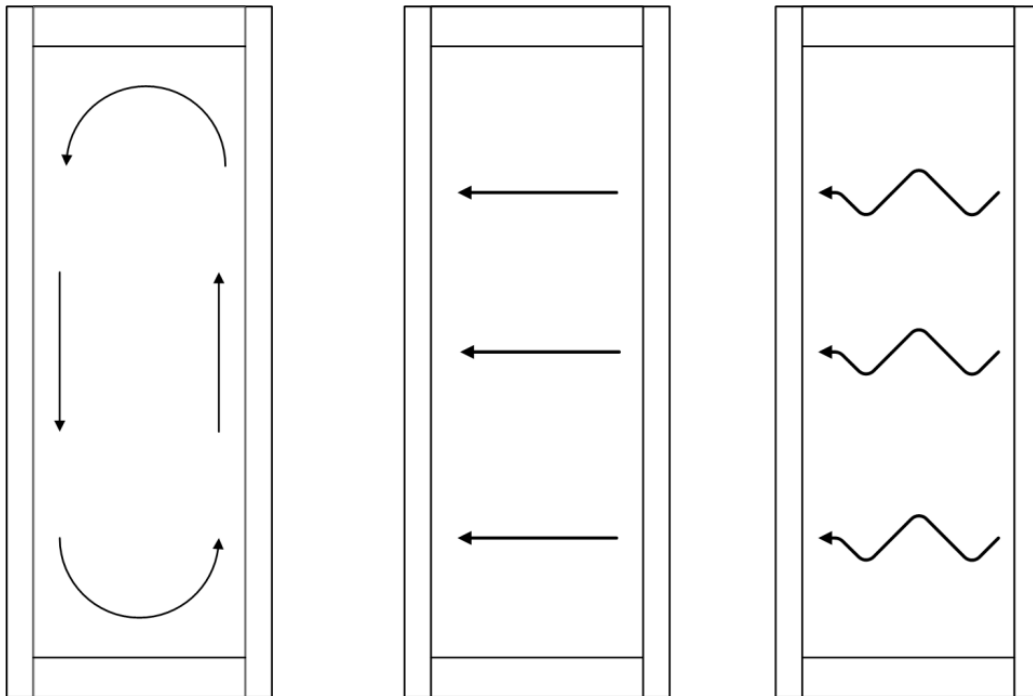

Figure 6. Illustration of convection, conduction and radiation in an IGU.

Convection occurs when there is a temperature gradient in a fluid. A flow starts in the fluid and in the interface to a surface, energy will be transferred either from a warmer surface to a colder fluid or from a warmer fluid to a colder surface, see Figure 6 [10]. The convection is reduced by a decrease of the space width and with higher density of the gas.

Conduction occurs when there is a temperature gradient in a material. The molecules transfer energy to the surrounding molecules without significant movement to equalize the temperature gradient [10]. The conduction occurs in the glass and the gas and is reduced by an increase of the space width and a higher density of the gas.

Radiation occurs when there is a temperature difference of two bodies where the warmer body emits energy to the colder body. In an IGU the radiation occurs between the glass panes, and is reduced with a low-emissivity coating, as described in Chapter 2.1.3.

3.2 1D-FE model

To obtain the temperature distribution through the IGU and thereby the mean temperatures in the cavities, which will determine the volume change of the gas and the bulging of the glass panes, a one dimensional model is used.

To model the heat flow through the IGU a constitutive relation is introduced. Fourier's law for heat conduction gives the flux $q = -k\frac{dT}{dx}$, where T is the temperature and k is the thermal conductivity. To include the effect of the convection and radiation a general heat resistance h is introduced, where $h = 1/k$ in Eq. (3.1). To read more about one dimensional heat flow, see pages 48-63 and 157-205 in [15].

$$q = -\frac{1}{h}\frac{dT}{dx} \tag{3.1}$$

A one dimensional linear element is modelled by the following equation:

$$h_n \begin{bmatrix} 1 & -1 \\ -1 & 1 \end{bmatrix} \begin{bmatrix} T_1 \\ T_2 \end{bmatrix} = \begin{bmatrix} Q_1 \\ Q_2 \end{bmatrix} \tag{3.2}$$

where Q is the total flux, T is the temperature and h_n the heat resistance for the glass panes, the cavities or the outside/inside which is described further in this chapter. An element can be a glass pane, a cavity or a surface on the outside or inside, and all elements are assembled to a global model, see Figure 7.
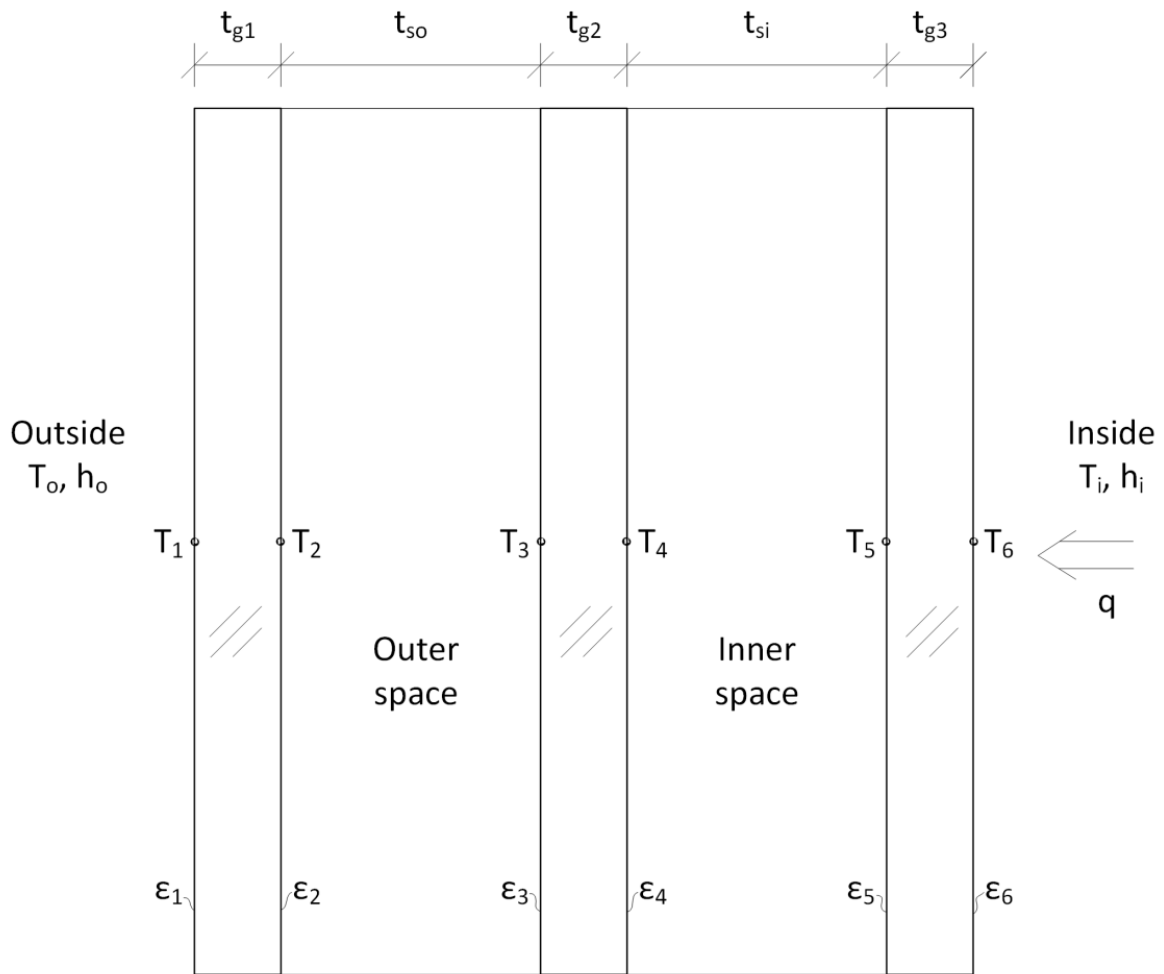

Figure 7. Model for a FE model in one dimension.T_n is the temperature, t_n is the thickness of the glass and spaces, ε_n is the emissivity of each surface.

14

The calculation method to be used is described in [17]. The method is considering the conductance, convection and radiation in the IGU.

3.2.1 Glass panes

In the glass panes, the heat transfer only consists of conduction. The heat resistance is obtained by:

$$h_{glass} = \frac{\lambda_{glass}}{t_{gn}} \tag{3.3}$$

where

$\lambda_{glass} = 0.81$ W/mK

t_n is the thickness of the glass panes [m]

3.2.2 Cavities

In the cavities, the heat transfer consists of conduction, convection and radiation. The heat resistance for the outer space is obtained by:

$$h_{cavity} = h_{cc} + h_r = \frac{Nu \cdot \lambda_{gas}}{t_{so}} + \sigma \cdot \frac{(T_2^2 + T_3^2)(T_2 + T_3)}{\varepsilon_{23}} \tag{3.4}$$

The convection and conduction part h_{cc} is obtained by:

λ_{gas} is the thermal conductivity of gas, see Table 6. [W/(mK)]

t_{so} is the width of the outer space, t_{si} is the width of the inner space. [m]

Nu is the Nusselt number describing the magnitude of convection in relation to the conduction. If $Nu = 1$, only conduction will occur in the cavity. The Nusselt number for natural convection in a closed space can be expressed by:

$$Nu = (1 + (C_1 \cdot Ra^{C_2})^{C_3})^{1/C_3} \tag{3.5}$$

where

$C_1 = 0.0227$, $C_2 = 0.438$ and $C_3 = 18$ are coefficients considering a closed space.

Ra is the Rayleigh number considering the properties of the gas, the distance of the space and the temperature difference between the surfaces.

$$Ra = \frac{\rho^2 \cdot g \cdot \beta \cdot \Delta T \cdot t_{so}^3 \cdot c_p}{\mu \cdot \lambda_{gas}} \tag{3.6}$$

where

g is the gravitational acceleration, 9.81 m/s^2.

β is the thermal expansion coefficient, $1/T_m$ for ideal gases, where T_m is the average temperature in the gas. [1/K]

15

ΔT is the temperature difference between the two surfaces in the closed space. [K]

c_p is the specific heat capacity of the gas, see Table 6. [J/(kgK)]

μ is the dynamic viscosity of the gas, see Table 6. [Pa·s]

ρ is the density of the gas. [kg/m³] The density is assumed to vary with the temperature. From $\rho = \frac{m}{V}$, $m = n \cdot M$ and the ideal gas law $pV = nR_cT$ [27], the density equation can be rewritten as:

$$\rho = \frac{m}{V} = \frac{n \cdot M \cdot p}{n \cdot R_c \cdot T_m} = \frac{M \cdot p}{R_c \cdot T_m} \tag{3.7}$$

where

M is the molecular mass of the gas, see Table 6. [kg/mol]

p is the pressure in the gas. [Pa]

R_c is the gas constant, 8.314 [J/mol·K]

The radiation part h_r is an expansion of Stefan Boltzmann's law, Eq.(3.8). For two parallel surfaces it will give h_r which is expressed in Eq.(3.4), where T_n are the temperatures on the surfaces [K], $\varepsilon_{23} = 1/(\frac{1}{\varepsilon_2} + \frac{1}{\varepsilon_3} - 1)$ where ε_2, ε_3 are the emissivity for the two surfaces facing each other. $\varepsilon = 0.837$ for annealed glass and $\varepsilon = 0.037$ for low-E glass.

$$q_r = \varepsilon \cdot \sigma \cdot T^4 \tag{3.8}$$

where

q_r is the flux of the radiation [W/m²].

σ is Stefan-Boltzmann's constant, 5.67·10⁻⁸ W/(m²K⁴).

ε is the emissivity.

T is the temperature [K].

All bodies in general receive and emit energy to other bodies. The radiation depends on temperature differences of the bodies and the emissivity of the bodies. The emissivity is a factor between 0 and 1 where an ideal black body would have 1. The intensity radiated from a body is obtained by the Stefan-Boltzmann law [10].

3.2.3 Outer and inner surfaces

At the outer and inner surface the heat transfer consists of convection and radiation. The heat resistance is obtained by:

$$h_{o,i} = \frac{1}{R} \qquad (3.9)$$

where R is the transfer resistance at the surface, on the outside $R_o = 0.04$ m²K/W while on the inside $R_i = 0.13$ m²K/W [10]. These may change when the IG units are in the Hotbox due to different magnitude in convection and radiation.

3.2.4 Solar radiation

Solar radiation heats up the IGU and the gas will expand which may lead to high stresses in the glass panes, see Figure 1.

The increase of temperature due to the solar radiation depends on the incidence angle of the solar radiation, the thickness of the glass panes and if there is a low-E coating on the surface. In Table 3, 4 and 5 the absorbance, the transmittance and the reflectance are shown for annealed glass and low-E glass. These factors are relatively constant for an incidence angle up to 45° where they change rapidly. The rapid change occurs because an increasingly amount of the solar radiation is reflected at the first glass pane surface [1].

The solar radiation that hits the atmosphere has an intensity of approximately 1370 W/m² [22]. The incoming solar radiation to the Earth surface in Sweden on a clear day is approximately 1090 W/m² since some of the radiation is reflected and absorbed in the atmosphere [10].

The incoming solar radiation is divided into components and the component perpendicular to the IGU's surface is designated as I_{eff} and calculated with Eq. (3.10) [10].

$$I_{eff} = I_0 \cdot \cos(\alpha) \qquad (3.10)$$

where

I_0 is the solar radiation intensity on the Earth surface in Sweden, 1090 W/m².

α is the angle between the sunbeams and the normal to the surface [°].

An assumption is made to always have the IGU towards the sun. Thereby the solar radiation is only divided into vertical components.

When an IGU is exposed to solar radiation some energy will reflect, some will transmit and some will be absorbed by the glass panes. In Figure 8 the transmittance, reflectance and absorbance is shown for an IGU with two glass panes.
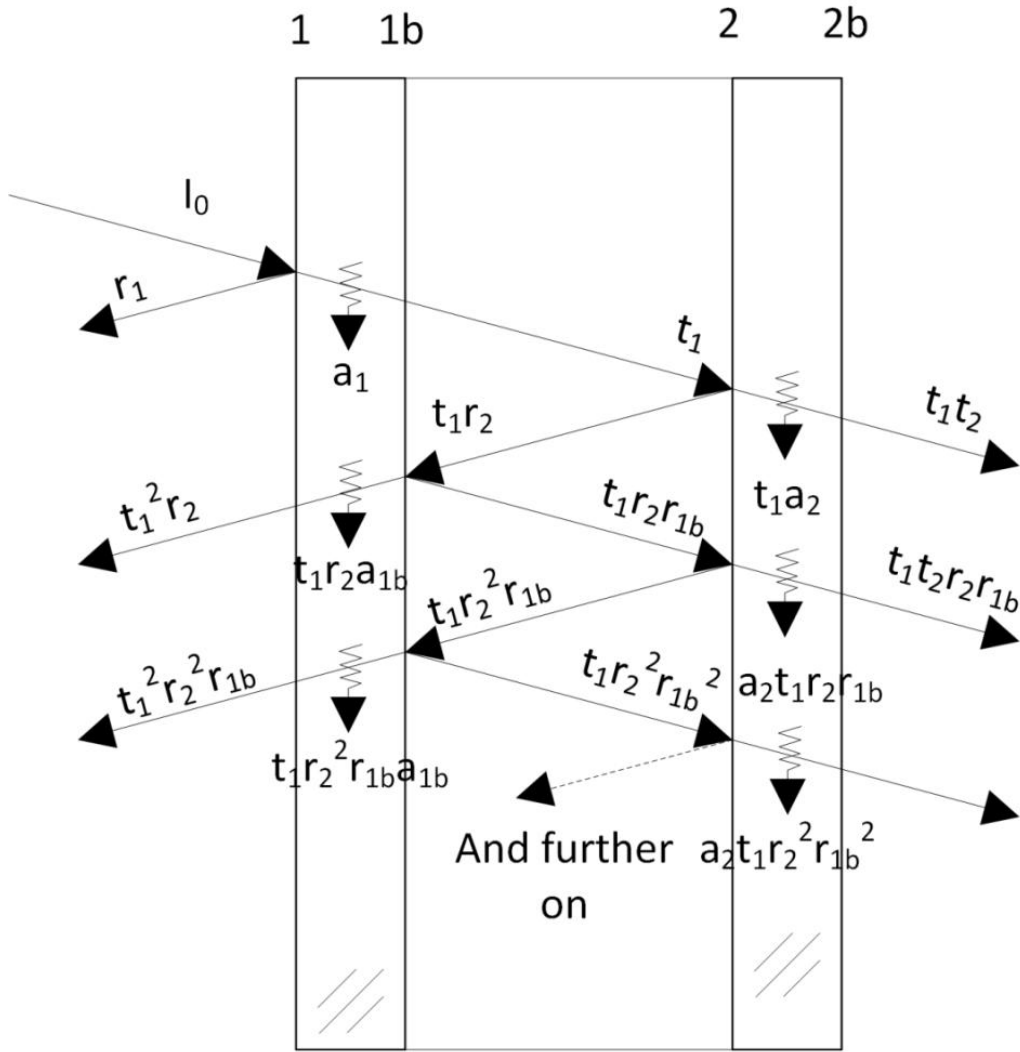
Figure 8. Transmittance (t), absorbance (a) and reflectance (r) in a two layer glass pane.

The total absorbance of the glass panes can be calculated by adding the absorbance of each hit as shown in Figure 8.

For a two glass IGU the first absorbance for the first glass is $I_{eff} \cdot a_1$. The second absorbance comes from reflected radiation at the second glass, $I_{eff} \cdot t_1 r_2 a_{1b}$. The next absorbance of the first glass comes from the once more reflected radiation at glass number two. The third absorbance is then $I_{eff} \cdot t_1 r_2^2 a_{1b} r_1$, see Figure 8. The total absorbance of the first glass pane in a two glass IGU is obtained by:

$$a_1 = I_{eff} \cdot \left(a_1 + a_{1b} t_1 r_1 (1 + r_{1b} r_2 + r_{1b}^2 r_2^2 + \cdots + r_{1b}^\infty r_2^\infty) \right)$$

$$= I_{eff} \cdot \left(a_1 + a_{1b} t_1 r_2 \sum_{k=0}^\infty (r_{1b} r_2)^k \right) = I_{eff} \cdot \left(a_1 + \frac{a_{1b} t_1 r_1}{1 - r_{1b} r_2} \right) \qquad (3.11)$$

The absorbance for the second glass is the radiation transmitted through the first glass added with the radiation reflecting between first and the second glass. The total absorbance of the second glass is obtained by:

$$a_2 = I_{eff} \cdot a_2 t_1 + I_{eff} \cdot a_2 t_1 \cdot r_{1b} r_2 + I_{eff} \cdot a_2 t_1 (r_{1b} r_2)^2 + \cdots + I_{eff} \cdot a_2 t_1 (r_{1b} r_2)^\infty$$

$$= I_{eff} \cdot a_2 t_1 \sum_{k=0}^{\infty} (r_{1b} r_2)^n = I_{eff} \cdot a_2 \frac{1}{1 - r_{1b} r_2} \tag{3.12}$$

When adding a third glass in the IGU the reflections become more but the absorbance can still be calculated with the process in Eq. (3.11) and (3.12).

The main absorbance of the outer glass pane comes primarily from the direct solar radiation but also from reflected radiation from the second and third glass panes.

The total absorbance of the first glass pane in a three glass IGU is:

$$a_{tot1} = I_{eff} \left(a_1 + a_{1b} \left(\frac{t_1 r_2}{1 - r_{1b} r_2} + \frac{t_1 t_2^2 r_3}{(1 - r_{1b} r_2)(1 - r_{2b} r_3)(1 - t_2^2 r_{1b} r_3)} \right) \right) \tag{3.13}$$

The absorbance for the second glass is the radiation transmitted through the first glass added with the radiation reflecting between the two glass panes. The absorbance also comes from reflected radiation from the third glass.

The total absorbance of the second glass pane in a three glass IGU is:

$$a_{tot2} = I_{eff} \cdot t_1 \left(\frac{a_2}{1 - r_{1b} r_2} + \frac{t_2 r_3 (a_{2b} + a_2 t_2 r_{1b})}{(1 - r_{1b} r_2)(1 - r_{2b} r_3)(1 - t_2^2 r_{1b} r_3)} \right) \tag{3.14}$$

The third glass will absorb energy from transmitted radiation through the second glass and from reflective radiation between the second and third glass.

The total absorbance of the third glass pane in a three glass IGU is:

$$a_{tot3} = I_{eff} \frac{t_1 t_2 a_3}{(1 - r_{1b} r_2)(1 - r_{2b} r_3)(1 - t_2^2 r_{1b} r_3)} \tag{3.15}$$

To verify the calculations a comparison is made by formulations of the solar radiation problem in [13]. The summation of the total transmittance, absorbance and reflectance will be 1. The total transmittance through the IGU is derived in [13] and obtained by:

$$T_{tot} = \frac{T_1 T_2 T_3}{(1 - R_{1b} R_2)(1 - R_{2b} R_3) - T_2^2 R_{1b} R_3} \tag{3.16}$$

And the total reflectance on the outside of the IGU is obtained by:

$$R_{ext} = R_1 + \frac{T_1^2 R_2 (1 - R_{2b} R_3) + T_1^2 T_2^2 R_3}{(1 - R_3 R_{2b})(1 - R_2 R_{1b}) - T_2^2 R_3 R_{1b}} \tag{3.17}$$

As the summation of transmittance, absorbance and reflectance is equal to 1,Eq. (3.13)-(3.15) were verified with the equations (3.16) and (3.17) in [13]. The value was almost the same with only a deviation of 0.1 % which concludes that the equations for calculating the absorption for each glass are good approximations. A bit higher deviation, 1% was found when a blind was installed but the equations are still very accurate.

For each glass pane the total absorption is added as an external heat source in the 1D-FE model.

3.2.5 Clear cold sky
On a cold clear night the warmer IGU will emit energy to the colder sky. The outer glass will in this case reach a lower temperature than the outside temperature.

The outer space has a theoretical temperature of 0 K (-273.15°C). To take this into consideration the IGU is assumed to have two thermal resistance factors on the outer surface. $R_o = 0.04$ m²K/W is the first, taking into consideration the convection and radiation on the outside. The second is the thermal resistance considering the radiation to the outer space. It is assumed that the IGU is affected by 50% of each. The heat resistance coefficient for the radiation to outer space can according to [10] be approximately calculated with:

$$h_{r,space} = \frac{1}{R_{space}} = 4 \cdot \varepsilon_{12} \cdot \sigma_s \cdot T_m^3 \tag{3.18}$$

where

$\varepsilon_{12} = \dfrac{1}{\frac{1}{\varepsilon_1} + \frac{1}{\varepsilon_2} - 1}$ where ε_1=0.837 for annealed glass, ε_2 is assumed to be 1 for the outer space.

T_m is the average temperature between the IGU and the outer space. [K]

The temperature is probably not that cold as 0 K and the emissivity is probably a bit lower for the outer space. Therefore this is only the theoretical value of how much the IGU radiate to a cold sky.

3.3 The finite element method
Physical phenomena could in engineering mechanics be complicated to solve by analytical methods. These problems are modelled by differential equations assumed to hold over a specific region. With the finite element method an approximate solution is carried out for an entire region. Specific rules divide the region into smaller parts (finite elements) and an approximated solution for each element is carried out. To receive a better solution of the problem the region is divided into smaller elements; the collection of the finite elements is

called mesh. With a finer mesh the approximated solution converges to the exact solution [15].

3.3.1 Abaqus/CAE

Abaqus/CAE is one of five core software product in Abaqus FEA. Abaqus/CAE is used for modelling and analysis of mechanical components and is also used for visualize the result of the finite element analysis. [28]

The cavities are modelled as fluid cavities in Abaqus/CAE. The fluid cavity is specified with a surface which has to entirely consist of finite elements. The boundary of the cavity is specified using an element-based surface covering the elements that surrounds the cavity with surface normals pointing inwards. The specified surface determines the volume of the gas and for this volume the gas properties are introduced. The gas is modelled as an ideal gas which means that the ideal gas law determines the pressure change of the gas due to the difference in current temperature and the initial temperature of the gas [29].

To solve the problem the Newton's method is used. Shortly the Newton's method is used to solve nonlinear equilibrium equations by iteration. To start the iteration a guess near the true solution must be made, if the guess is good the solution after each iteration will converge to the true solution. In Abaqus/CAE this method is applied when the NLGEOM command is used for non-linear geometry. [30]

3.4 Python

Python is a programming language that supports multiple programming paradigms which means that Python can support other different programming languages. [31]

All the analysing models are written as a Python script for the possibility of sending data between the programs and run Abaqus/CAE through the script which makes it possible to do multiple analyses consecutive.

3.5 European standard

The design values of strength for annealed and toughened glass are obtained by the European standard. Characteristic values and factors are found in [8].

3.5.1 Design value of strength for annealed glass

The design value of strength for annealed glass is calculated by:

$$f_{g;d} = \frac{k_{mod} k_{sp} f_{g;k}}{\gamma_{M;A}} \tag{3.19}$$

where

$f_{g;k}$ is the characteristic value of bending strength for annealed glass, 45 MPa.

$\gamma_{M;A}$ is the material partial factor, 1.8 for annealed glass.

k_{sp} is the factor for glass surface profile, 1.0 for float glass.

k_{mod} is the factor for load duration obtained by:

$$k_{mod} = 0.663t^{-\frac{1}{16}} \tag{3.20}$$

where

t is the load duration in hours.

t is assumed to be 3 hours. The maximum or minimum temperature, which is the factor affecting the stresses in the IGU the most, is assumed to last approximately 3 hours in this work. Inserting this into Eq. (3.20) gives:

$$k_{mod} = 0.663 \cdot 3^{-\frac{1}{16}} = 0.619$$

Insertion of values in Eq. (3.19) gives the design value of strength for annealed glass:

$$f_{g;d} = \frac{k_{mod}k_{sp}f_{g;k}}{\gamma_{M;A}} = \frac{0.619 \cdot 1.0 \cdot 45}{1.8} = 15.48 \text{ MPa}$$

3.5.2 Design value of strength for prestressed glass

The design value of strength for toughened/prestressed glass is calculated by:

$$f_{g;d} = \frac{k_{mod}k_{sp}f_{g;k}}{\gamma_{M;A}} + \frac{k_v(f_{b;k} - f_{g;k})}{\gamma_{M;v}} \tag{3.21}$$

where

$f_{g;k}$, $\gamma_{M;A}$, k_{mod} and k_{sp} has the same values and are described in previous section.

$\gamma_{M;v}$ is the material factor for surface prestress, 1.2 for surface prestressed glass.

$f_{b;k}$ is the characteristic value of bending strength of prestressed glass, 120 MPa for float glass.

k_v is the factor of strengthening of pressed glass, 1.0 horizontal toughening.

Inserting values in Eq. (3.21) gives the design value of strength for toughened glass:

$$f_{g;d} = \frac{k_{mod}k_{sp}f_{g;k}}{\gamma_{M;A}} + \frac{k_v(f_{b;k} - f_{g;k})}{\gamma_{M;v}} = 15.48 + \frac{1.0 \cdot (120 - 45)}{1.2} = 15.48 + 62.50$$
$$= 77.98 \text{ MP}$$

4 Experimental Analysis

Experimental analyses were made in a Hotbox which is a climate chamber with a wall of cellular plastic dividing the Hotbox into two rooms, see Figure 9. The temperature in each chamber was set to 22°C respectively -20°C. The cellular plastic wall had a hole with the dimensions 1.2x2.4 m. The IG units were placed in the hole in the wall with the boundaries sealed with cellular plastic to reduce the thermal bridge effect.
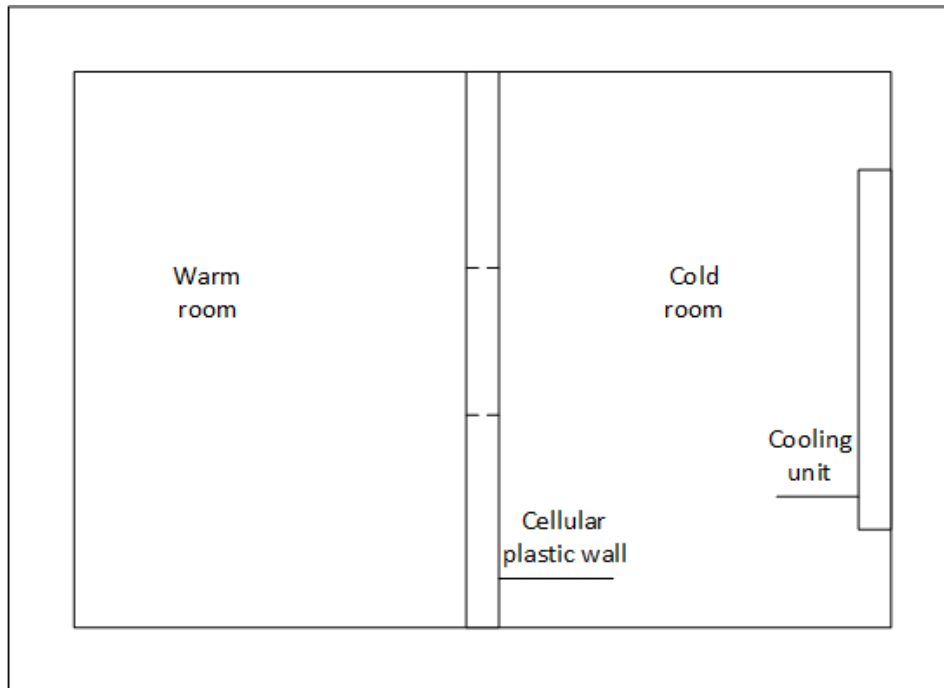

Figure 9. Illustration of the Hotbox.

4.1 Manufacturing

IG units with different geometries were manufactured. Most of the IG units had the width and height of 1.2 m to fit in the hole of the cellular plastic wall, but two were manufactured with different dimensions. The glass thicknesses were mostly 4 mm (3.8 mm). But one was tested with an outer glass thickness of 6 mm (5.8 mm). The space distances were varied for each IGU. For most cases, one parameter was changed for the different IG units to study the effect on the bulging and the temperature distribution through the IG units. The manufactured IG units are shown in Table 7.

IGU	Dimensions [mm]		Glass thickness[1] [mm]			Space distance [mm]		Gas content	
	Height	Width	Outer	Middle	Inner	Outer	Inner	Outer	Inner
1	1200	1200	6LE	4	4LE	22	16	Air	90% Ar
2	1200	1200	4LE	4	4LE	24	24	90% Ar?	90% Ar?
3	1200	1200	4LE	4	4LE	22	16	90% Ar	90% Ar
4	600	600	4LE	4	4LE	24	24	90% Ar?	90% Ar?
5	1800	1200	4LE	4	4LE	22	16	90% Ar	Air

Table 7. IG units manufactured for experimental tests.
[1]LE=Low-emissivity glass, coating towards the space.

To measure the temperature at the glass surfaces, thermocouple wire was used. The wire consists of two threads which were peeled and soldered together in a connection point at the end of the wire. At the other end a thermocouple connector is attached. This type of thermocouple wire and connector is of type T, tolerance class 1 which means a tolerance of ± 0.5°C is allowed [25].

The IG units were manufactured as described in Chapter 2.6 but with a thermocouple wire attached on the centre of the middle glass pane. The thermocouple wire was attached with transparent tape so that the radiation would not affect the temperature. A hole in the spacer had to be done for the thermocouple wire which resulted in a gas content that was a bit unsure due to a more complicated sealing process. A gas content of 90% argon was the aim but some cavities might have less or were totally filled with air.

The atmospheric pressure on the manufacturing day was 100.9 kPa and the temperature in the production site was 20°C [19] which was used as the initial values for the gas.

4.2 Performance of tests

The IGU was placed in the Hotbox, starting with the largest IGU and continuing with the smaller ones. The rest of the hole was filled with cellular plastic and sealed with insulation at the edges. Thermocouple wires were attached with transparent tape on the outer surfaces of the IG units. The thermocouple wires were connected to a meter cabinet that was connected to a computer that logged the temperatures, see Figure 10.

The temperature in the warm and cold room was set to 22°C respectively -20°C. These temperatures were not reached exactly due to some leakage and that the cooling unit did not have the full efficiency. When the temperatures were stabilised the bulging was measured across both diagonals on each side of the IG units with an aluminium straight edge and a digital calliper. The spaces between the glass panes in the IG units were measured with a digital laser.

Figure 10. Left: Meter cabinet for thermocouple wires. Right: Installed IGU in Hotbox.

Three tests were made in the Hotbox:

- Test 1: the IG units were placed in the Hotbox with different temperatures on each side.
- Test 2: the IG units were placed in the cold room with cool temperatures on both sides.
- Test 3: the IG units were placed in the laboratory hall with room temperatures on both sides.

Figure 11 shows the temperature distribution in IGU 1 over the time when it was placed in the cellular plastic wall in the Hotbox.
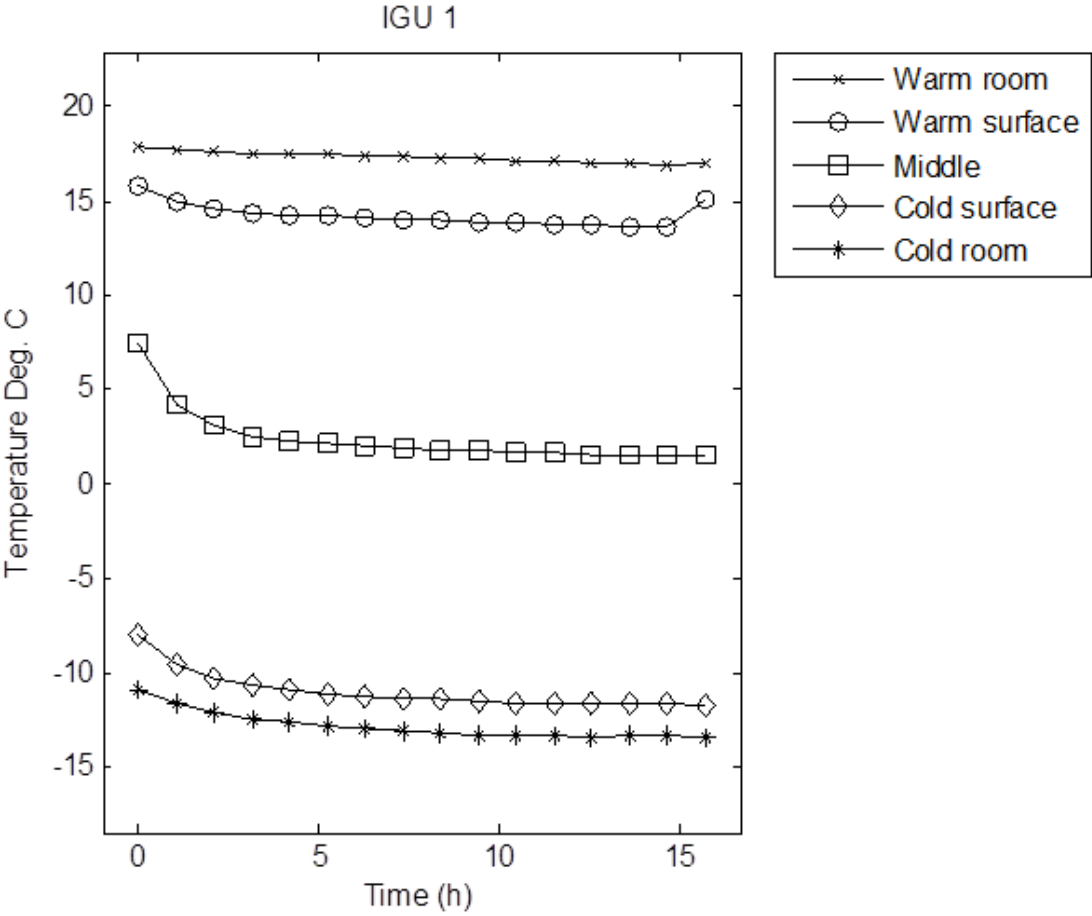
Figure 11. Temperature distribution of IGU 1 when placed in cellular plastic wall.

The bulging was measured after approximately 14 hours for this IGU. The temperature distributions for the other IG units are presented in Appendix A.

When the temperatures in the IG units stabilised for each test, the bulging was measured. The total bulging as shown in Figure 12 was measured with the calliper and calculated from the laser measurements. The total bulging was later compared with the FE-model.

Figure 12. Illustration of the total bulging of the IGU.

The total bulging in the middle of the IGU is $\delta_1 + \delta_2$ as is shown in Figure 12.

Due to the time constraints while performing the experimental analyses the bulging of the IG units were not measured in all tests.

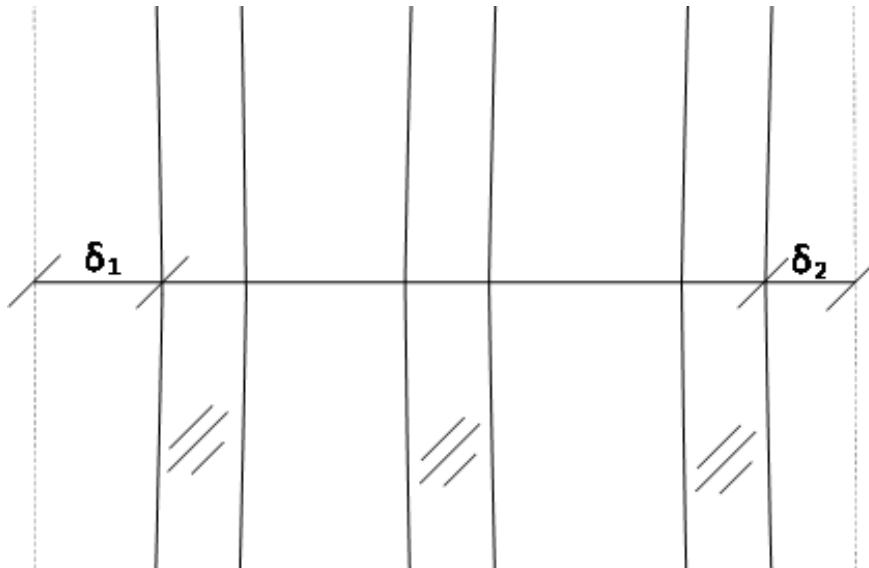When the IG units were in the cold room (Test 2) the thermocouple wires were calibrated. The wires that were placed in the middle of the IG units and those two that were placed on the surfaces were calibrated to the wire that measured the temperature in the cold room. The temperatures measured by the thermocouple wires varied with approximately ±0.5°C. Due to the time constraints the thermocouple wire for the one in the middle of IGU 1 was not calibrated, but this was assumed to not vary more than ±0.5°C. For calibrated values see Appendix A.

4.3 Results

4.3.1 Test 1
In Test 1 the IG units were placed in the Hotbox with different temperatures on each side.

In Table 8 the testing time, the atmospheric pressure at the testing day and the stabilised calibrated temperatures for the IG units are presented.

IGU	Testing time [h]	Cold room [°C]	Cold glass surface[°C]	Middle glass [°C]	Warm glass surface [°C]	Warm room [°C]	Atm. p. [kPa]
1[1]	14	-13.4	-11.6	1.6	13.7	17.0	101.7
2	64	-14.0	-12.1	3.7	14.6	17.7	101.4
3	5	-13.5	-11.9	1.9	14.3	17.7	101.2
5	21	-10.6	-9.2	5.6	19.3	23.2	101.3

Table 8 Converge temperatures of the IG units.
[1]Temperature not calibrated, could vary ±0.5°C.

27

The obtained displacement of the glass panes, the decrease of space distances and the total bulging are presented in Table 9.

Calliper				Laser		
IGU	Glass displacement [mm]		Total bulging in middle [mm]	IGU	Decrease of spaces [mm]		Total bulging in middle [mm]
	Outer	Inner			Outer	Inner	
1	3.1	5.7	8.8	1	5.5	2.7	8.3
2	6.3	4.5	10.8	2	9.3	1.8	11.0
3	6.0	5.1	11.1	3	7.7	2.7	10.4
4				4			
5	6.7	3.4	10.2	5	6.5	3.3	9.7

Table 9. Displacement of glass, reduction of cavity and total bulging in the middle for two measuring techniques, Test 1.

The standard deviations for the measurements were between 0.1-0.5 mm and are shown in Appendix A.

4.3.2 Test 2

In Test 2 all the IG units were placed in the cold room with -10.15°C where the atmospheric pressure that day was 101.6 kPa [19].

The obtained displacement of the glass panes, the decrease of space distances and the total bulging are presented in Table 10.

Calliper				Laser		
IGU	Glass displacement [mm]		Total bulging in middle [mm]	IGU	Decrease of spaces [mm]		Total bulging in middle [mm]
	Outer	Inner			Outer	Inner	
1				1			
2	8.1	7.0	15.1	2	9.5	4.7	14.2
3	6.8	6.3	13.1	3	8.1	4.8	12.9
4	5.9	5.7	11.5	4			
5	7.0	5.8	12.8	5	7.0	5.1	12.1

Table 10. Displacement of glass, reduction of cavity and total bulging in the middle for two measuring techniques, Test 2.

The standard deviations for the measurements were between 0.1-0.3 mm and are shown in Appendix A.

4.3.3 Test 3

In Test 3 the IG units were placed in the laboratory hall with 20.9°C where the atmospheric pressure that day was 102.2 kPa. [19]

The IG units were covered by opaque plastic so that the temperature would not increase due to the solar radiation. The temperature in the middle glass was measured to make sure the temperature in the IGU had stabilised.

The obtained displacement of the glass panes, the decrease of space distances and the total bulging are presented in Table 11.

Calliper				Laser		
IGU	Glass displacement [mm]		Total bulging in middle [mm]	IGU	Decrease of spaces [mm]		Total bulging in middle [mm]
	Outer	Inner			Outer	Inner	
1	1.4	2.9	4.3	1	2.2	1.8	3.9
2	3.5	2.2	5.7	2	5.6	-0.2	5.4
3	4.3	2.5	6.8	3	4.5	1.8	6.3
4	1.6	1.6	3.2	4	2.1	1.8	3.9
5	3.1	1.5	4.6	5	2.5	2.0	4.5

Table 11. Displacement of glass, reduction of cavity and total bulging in the middle for two measuring techniques, Test 3.

The standard deviations for the measurements were between 0.1-0.2 mm and are shown in Appendix A.

4.4   Discussion of experimental analyses

Since the Hotbox was relatively sealed, the pressure in the cold room decreased due to the temperature change but since the door was opened before the measurements were carried out an assumption was made that the pressure in the Hotbox equalized and became the same as the atmospheric pressure outside of the Hotbox.

When comparing the results from Test 1 some interesting findings were made. IGU 1 and IGU 3 had identical geometry except that the outer glass thickness in IGU 1 was 6 mm instead of 4 mm and that the outer cavity in IGU 1 was filled with air instead of argon. The outer glass in IGU 1 had a smaller displacement than the inner glass. When the thicknesses were the same for all glass panes in the IGU it gave a larger displacement of the outer glass which was found for all of the other IG units in Test 1, see Table 9. When the thickness of one glass pane was bigger it led to a larger bulging of the other glass panes in the IGU.

When the IG units were placed in the laboratory hall in Test 3 a quite large bulging was measured, see Table 11. The temperature was a bit higher than the initial value of the gas which would give an outwards bulging while the atmospheric pressure was higher than the initial pressure in the gas but the difference was not large enough that the bulging would be 1-4 mm on each side of the IG units. A conclusion was that a remaining bulging occurred after the IG units had been in the Hotbox and exposed to temperature loads. Probably some plastic deformations occurred in the sealant or the spacer but it has to be further investigated. The bulging of the IG units should have been measured directly after manufactured, before they were placed in the Hotbox and after they had been in the Hotbox.

If measurements like this will be made in the future a suggestion is to measure vertically and horizontally with the aluminium straight edge and the calliper. The bulging measurements will then be more accurate if the IG units are a bit skewed or curved. Also, the thickness of the IG units around the edges should be measured to investigate the residual bulging.

When the experimental analyses were compared to the model the residual bulging was neglected.

4.5 Calibration of 1D-FE model

Since the inner and outer convection and radiation is unknown in the Hotbox, new R_o and R_i were calculated from the temperatures in Table 8. The thermal resistance in the Hotbox could be determined from the known temperatures in each room and the temperatures of the facing surfaces.

The flux through the IGU was obtained by Eq.(2.25) in [10]:

$$q = \frac{T_o - T_i}{\sum R} \tag{4.1}$$

where

T_o and T_i is the outer and inner temperature. [K]

$\sum R$ is the total transfer resistance. [m²K/W]

With constant flux through the IGU, the flux is calculated from known temperatures in the outside room and on the outer glass surface, and the transfer resistance on the outside surface.

$$q = \frac{T_o - T_1}{R_o} \tag{4.2}$$

With constant flux q and by combining Eq.(4.1) and Eq.(4.2) gives:

$$\frac{T_o - T_1}{R_o} = \frac{T_o - T_i}{\sum R}$$

with $U = \frac{1}{\sum R}$ [10]:

$$R_o = \frac{T_o - T_1}{U \cdot (T_o - T_i)} \tag{4.3}$$

Similar calculations on the inside, R_i is obtained by:

$$R_i = \frac{T_6 - T_i}{U \cdot (T_o - T_i)} \tag{4.4}$$

where

U is the total heat resistance. [W/m²K]

Since U is a function of R an iteration was done until the temperatures were the same as in the measurements.

The thermal resistance for the IG units in Test 1 became:

IGU	R_o [m²K/W]	R_i [m²K/W]
1	0.08	0.15
2	0.09	0.14
3	0.07	0.16
4		
5	0.05	0.15
Average	0.07	0.15

Table 12. R_o and R_i for the different IG units in the Hotbox.

Average outer heat resistance was 0.07 m²K/W for the cold room and the inner heat resistance was 0.15 m²K/W for the warm room.

A comparison was made for these calculated values with the traditional used R-values outside and inside (0.04 and 0.13 m²K/W). R_i in the Hotbox was very close, only a bit higher. R_o was higher in the Hotbox and this was probably due to that the convection in the cold room is lower than a normal day outside.

The thermal resistance of the external surfaces according to [10] is:

$$R = \frac{1}{\alpha_r + \alpha_c} \tag{4.5}$$

where

α_r is heat transfer coefficient for radiation and α_c is the heat transfer coefficient for convection. [W/m²K]

The emissivity was unknown on both sides of the IG units in the Hotbox. An assumption was made that the emissivity was approximately 0.9 for the walls in the Hotbox. The average temperature in the two rooms were assumed to be 290 K in the warm room and 260 K in the cold room which it were for three of the tested IG units. From Eq.(4.5) α_s and α_c is obtained:

On the warm side the heat transfer coefficient is:

$$\alpha_r + \alpha_c = \frac{1}{R_i} = \frac{1}{0.15} = 6.6 \text{ W/m}^2\text{K}$$

According to [10] α_s is approximately:

$$\alpha_r = 4 \cdot \sigma_s \cdot \varepsilon_{12} \cdot T_m^3 = 4 \cdot 5.67 \cdot 10^{-8} \cdot \frac{1}{\frac{1}{0.837} + \frac{1}{0.9} - 1} \cdot 293^3 = 4.2 \text{ W/m}^2\text{K}$$

The heat transfer coefficient for convection is then:

$$\alpha_c = \frac{1}{R_i} - \alpha_r = 6.6 - 4.2 = 2.4 \text{ W/m}^2\text{K}$$

On the outside (in the cold room) the heat transfer coefficient is obtained with the same calculations:

$$\alpha_r + \alpha_c = \frac{1}{R_o} = \frac{1}{0.07} = 13.6 \text{ W/m}^2\text{K}$$

$$\alpha_r = 4 \cdot 5.67 \cdot 10^{-8} \cdot \frac{1}{\frac{1}{0.837} + \frac{1}{0.9} - 1} \cdot 260^3 = 3.1 \text{ W/m}^2\text{K}$$

$$\alpha_c = \frac{1}{R_o} - \alpha_r = 13.6 - 3.1 = 10.5 \text{ W/m}^2\text{K}$$

Comparing this with the calculated α_c for natural convection in a room gives [10]:

$$\alpha_c = C \cdot \sqrt[4]{T_1 - T_2} \approx 2 \cdot 1.3 \approx 3 \text{ W/m}^2\text{K}$$

The α_c in the warm room was calculated to be 2.4 W/m²K which was reasonable when compared it with natural convection in a room which were approximately 3 W/m²K. However the α_c in the cold room was approximately 10.7 W/m²K which did not occur due to natural convection. There had to be some forced convection e.g. from the cooling unit.

The temperatures in the middle glass were calculated with the 1D-FE model with the new R-values, shown in Table 12 and the results are shown in Table 13.

IGU	Measured temperatures [°C]	1D-FE model temperatures [°C]
1	1.6	-0.6
2	3.7	1.1
3	1.9	0.7
4	-	-
5	5.6	3.3

Table 13. Temperature in the middle glass, measured and modelled values.

For the larger IG units the measured values showed a higher temperature in the middle glass than obtained from the 1D-FE model. When the glass panes bulged inwards in the Hotbox, the heat flux through the IG units changed which increased the temperatures in the middle glass for all IG units. This is probably due to the reduced space, that the convection, conduction and radiation become different when the glass panes are bulging inwards. A conclusion was made that the model without compensation for a decreased distance in the cavities shows a lower temperature than the measured temperature.

5 FE Model

A finite element model was created in Abaqus/CAE to determine the displacements and stresses in the glass panes of the IGU. The FE-model was implemented as a Python script in order to automate the calculations. Automatisation of the calculations made it possible to do a large number of analyses of IG units with different configurations and loads. The computing time for each analysis was therefore of major importance.

5.1 Geometry and material

The model was created as one part with cavities, with a simplified geometry and the cross section can be seen in Figure 13. Partitions of the part were made to obtain the glass panes, the spacers and the sealants. The thicknesses of the butyl layers were set to 0.3 mm and the thicknesses of the polysulphide and the spacers were set to 6 mm. The other dimensions could vary in the model. The cavities were defined as pneumatic fluid by specify the surfaces around the fluid. A reference node was created for each cavity to set the initial values, and later to obtain the temperature when the IGU is installed.
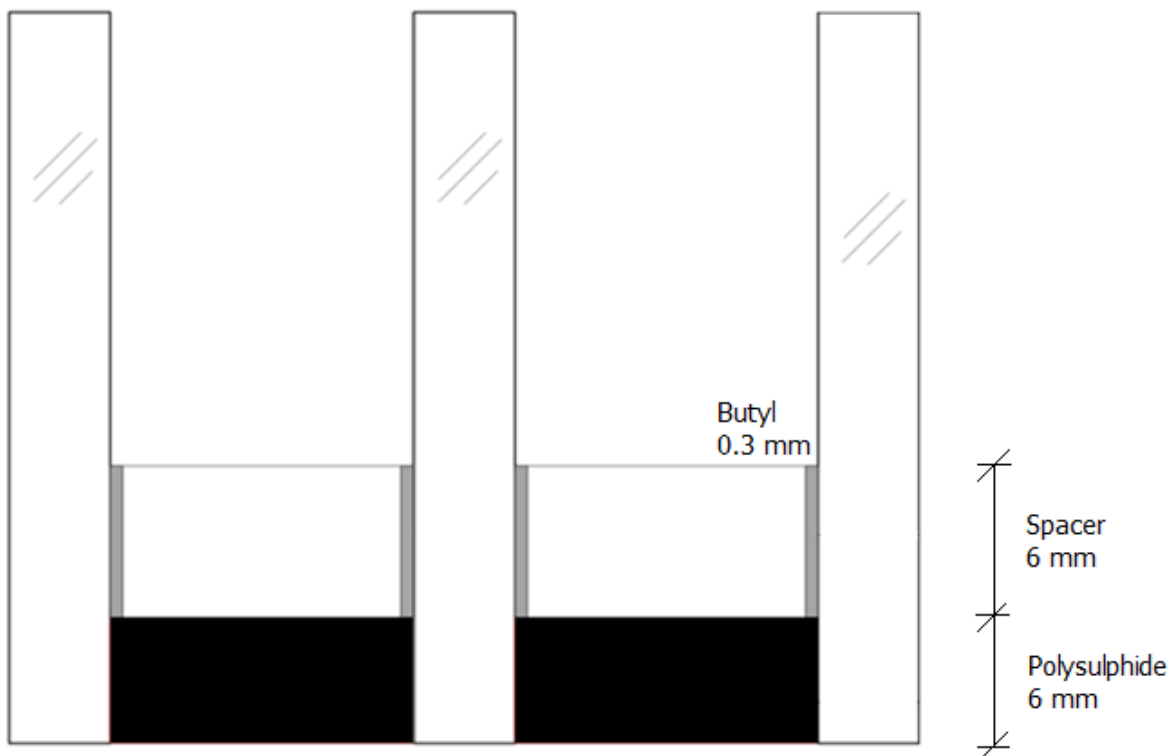

Figure 13. Geometry of model.

The materials used in the model are described in Chapter 2. The Young's modulus of the sealants had to be studied to see its effect on the bulging since the Young's modulus can vary with the temperature.

The Young's modulus of butyl can vary between 2.13-4.25 MPa and the Young's modulus of polysulphide can vary between 1.6-2.7 MPa due to the temperature in the sealants, see Figure 5. A study was made to investigate the effect of varied Young's modulus in the sealants' on the resulting deformations.

33

A 1.2x1.2m^2 IGU was used when the change of the Young's modulus was studied to see the effect of the displacements on the glass panes. A 0.6x0.6m^2 IGU was used to see the Young's modulus effect on the stresses in the glass panes. Both the IG units had the inner space of 22 mm and the outer space of 16 mm. The temperature inside and outside was set to 20°C and -20°C, and the atmospheric pressure difference was 3 kPa.

When the Young's modulus for both sealants was assigned the lowest value the displacement in the outer glass was 3.27 mm and the stress in the outer glass was 16.0 MPa for the different IG units. For the highest value of Young's modulus for the sealants, the displacement and the stress only became 0.01 mm and 0.2 MPa higher. These results concluded that the Young's modulus in these ranges had a negligible influence on the displacements and stresses in the IGU. The Young's modulus was therefore set to 2.13 MPa for the butyl and 1.6 MPa for the polysulfide.

5.2 Finite elements
The displacements in the elements were assumed to vary quadratic therefore 20 node brick elements with reduced integration were chosen. For further reading about element types, see chapter 19 in [15].

5.3 Loads and boundary conditions
The loads which affects the bulging of the IGU originates from the temperature changes in the cavities and the difference between the initial pressure in the cavities and the atmospheric pressure. The pressure changes in the cavities are calculated with the ideal gas law. The temperatures in the cavities were calculated in the 1D-FE model or from the calculated average temperatures from the measurements. The pressure difference was acting on the outer and inner surfaces of the IGU as uniformly distributed load, see Figure 14.
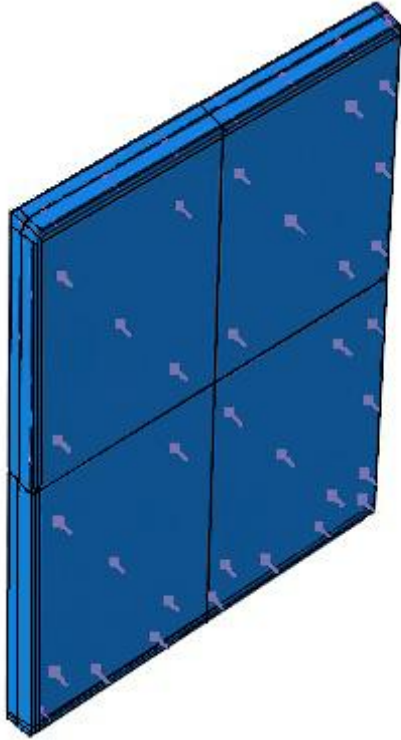
Figure 14. Pressure on IGU.

The boundary conditions were set so no restraints were imposed on the deformations but the rigid body displacements were constrained. The boundary conditions were imposed on the middle glass in three points, see Figure 15.
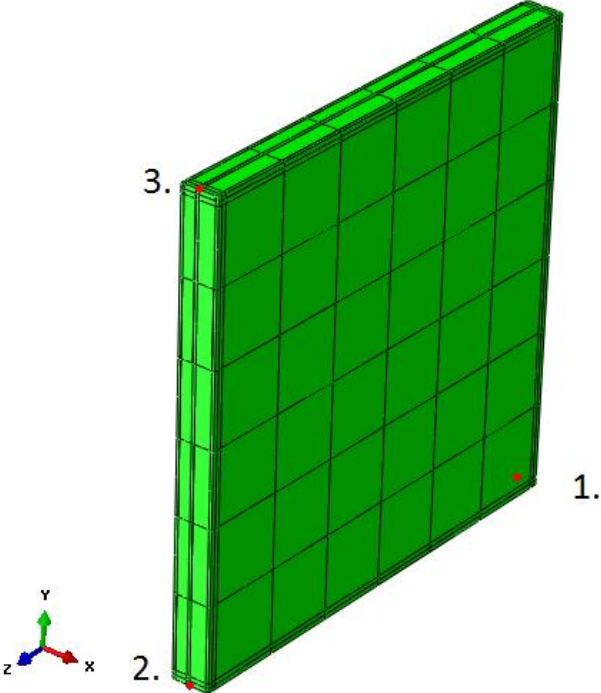

Figure 15. Points for prescribed displacements in model

The boundary conditions were set as in Table 14.

Point	Prescribed boundary condition
1	x,y- direction
2	x,y,z-direction
3	x,z-direction

Table 14. Prescribed boundary conditions.

5.4 Mesh convergency

As mentioned previously the computing time was of major importance. With a fine mesh the solution, i.e. the displacements and stresses in the glass, will converge to the true value but with the cost of computing time. A mesh convergence study was made by changing the element size in the yz-plane while keeping the mesh in z-direction to one element for every layer. Thereafter the mesh size in the yz-plane was kept constant and the element size in x-direction was changed.

The stresses were checked from an IGU with dimensions 0.6x0.6m^2 and the displacements were an IGU with the dimensions 1.2x1.2m^2. Both distances of the cavities were set to 16 mm and the glass thicknesses for all three glass panes were set to 3.8 mm. The inner temperature was set to 20°C and the outer temperature was set to -30°C. A pressure of 3 kPa higher than the initial pressure in the cavity was assumed to act on the IG units.
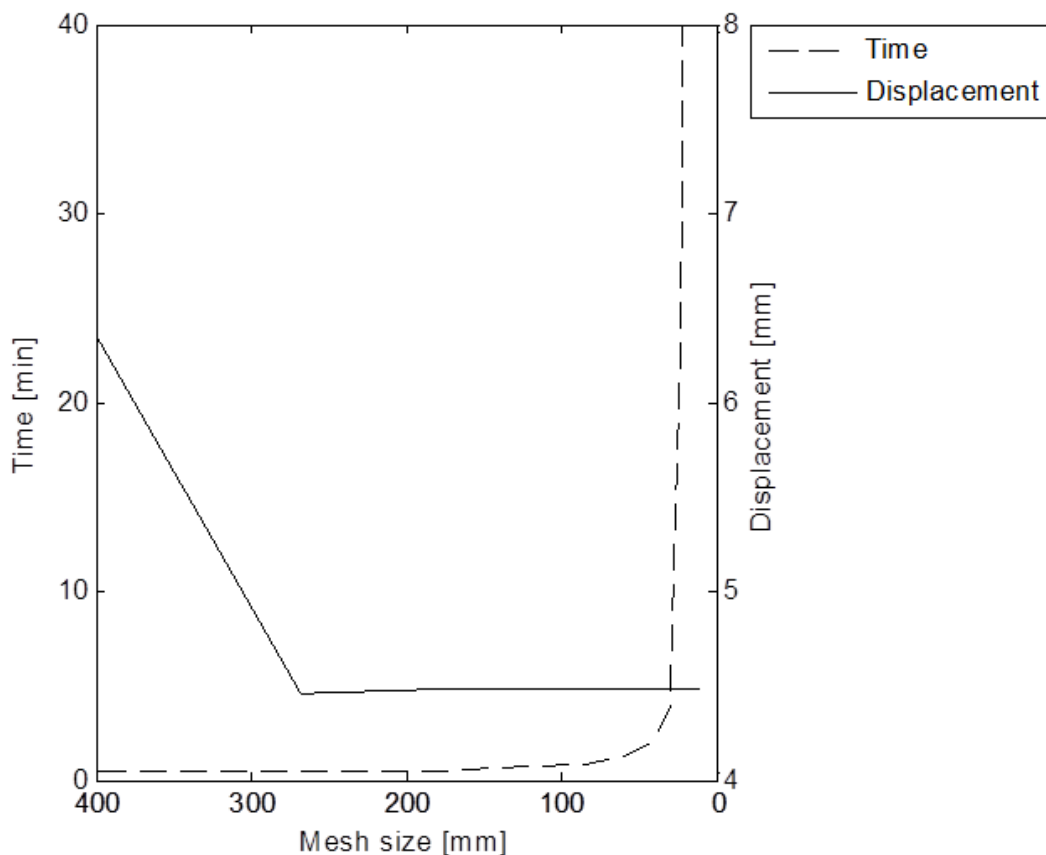

Figure 16. Displacement/time in the outer glass as function of mesh size.

In Figure 16 the displacement in the outer glass is shown for the $1.2 \times 1.2 \text{m}^2$ IGU when the mesh size was varied in the yz-plane. As can be seen in the figure, there were small changes for the displacement but the analysing time increased rapidly when an element size smaller than 40 mm was used.
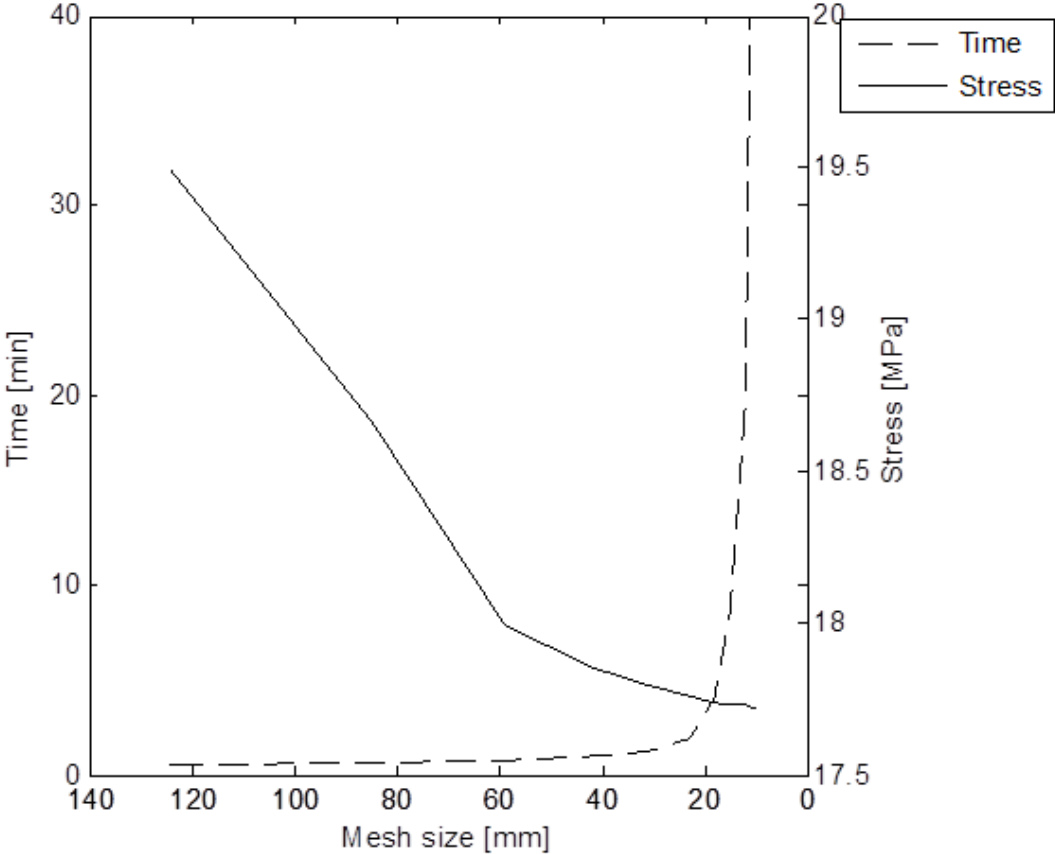

Figure 17. Stress/time in the outer glass as a function of the mesh size.

In Figure 17 the stresses in the outer glass is shown for the $0.6 \times 0.6 \text{m}^2$ IGU when the mesh size was varied in the yz-plane. The analysing time increased rapidly for an element size smaller than 20 mm.

The stress was decisive for the computing time, therefore the $0.6 \times 0.6 \text{m}^2$ IGU was also analysed when the element size in the x-direction was varied with the same load.

One element for all layers resulted in 17.846 MPa in the outer glass pane. With one element in the glass panes and two elements in the spaces resulted in 17.854 MPa. With two elements in the glass panes and three elements in the spaces resulted in 17.842 MPa. A larger number of elements in the x-direction did not affect the result significantly, therefore one element in each layer was chosen.

An element size in the xy-plane of 40 mm was chosen. The displacements converged for this size and the stresses convergence was considered to be sufficient and the computing time was still short.

37

6 Comparisons with Experimental Analyses

To verify the model and to investigate its agreement with measurements, the IG units that were tested in the Hotbox where modelled. The geometries and the atmospheric pressure that were modelled are shown in Table 7. The average temperatures in the cavities used in the model were calculated from Table 8 for Test 1. The temperature for Test 2 was -10.15°C on both sides of the IGU and an atmospheric pressure of 101.6 kPa, 0.7 kPa higher than the initial value of 100.9 kPa. For Test 3 the temperature was 20.9°C on both sides of the IGU and an atmospheric pressure of 102.2 kPa, 1.3 kPa higher than the initial value of 100.9 kPa.

6.1 Results

6.1.1 Test 1
The bulging for each glass pane and the total bulging for IG units with differing temperatures on the different sides are presented in Table 15.

IGU	Displacement [mm]			Total bulging in middle [mm]
	Outer	Middle	Inner	
1	2.32	-2.25	-3.92	6.24
2	3.82	-0.92	-3.18	7.00
3	3.35	-1.02	-2.57	5.92
4	-	-	-	-
5	3.64	-1.09	-2.80	6.44

Table 15. Displacement of the glass and the total bulging in the middle for modelled Test 1.

6.1.2 Test 2
The bulging for each glass pane and the total bulging for IG units with -10.15°C on both sides are presented in Table 16.

IGU	Displacement [mm]			Total bulging in middle [mm]
	Outer	Middle	Inner	
1				
2	5.70	0.00	-5.70	11.41
3	4.77	-0.60	-4.49	9.26
4	4.08	0.00	-4.08	8.15
5	4.83	-0.59	-4.51	9.34

Table 16. Displacement of the glass and the total bulging in the middle for modelled Test 2.

6.1.3 Test 3

The bulging for each glass pane and the total bulging for IG units with 20.9°C on both sides are presented in Table 17.

IGU	Displacement [mm]			Total bulging in middle [mm]
	Outer	Middle	Inner	
1	0.26	-0.22	-0.57	0.83
2	0.53	0.00	-0.53	1.06
3	0.44	-0.04	-0.40	0.84
4	0.38	0.00	-0.38	0.77
5	0.44	-0.05	-0.40	0.84

Table 17. Displacement of the glass and the total bulging in the middle for modelled Test 3.

When the FE-model was compared with the experimental analyses the difference between Test 1 and Test 2 were made with Test 3 to neglect the residual deformations which were obtained in the experimental analyses in Test 3.

IGU	Comparison of tests	FE-Model [mm]	Measured		Difference	
			Calliper [mm]	Laser [mm]	Model-Calliper [mm]	Model-Laser [mm]
1	Test1-Test3	5.4	4.6	4.3	0.8	1.1
2	Test1-Test3	5.9	5.1	5.6	0.8	0.3
	Test2-Test3	10.3	9.4	8.8	0.9	1.5
3	Test1-Test3	5.1	4.3	4.1	0.7	1.0
	Test2-Test3	8.4	6.3	6.6	2.1	1.8
4	Test2-Test3	7.4	8.3		-0.9	
5	Test1-Test3	5.6	5.6	5.3	0.0	0.3
	Test2-Test3	8.5	8.2	7.7	0.3	0.8

Table 18. Comparison between model and the two measuring techniques calliper and laser.

When the total bulging of the FE-model was compared with the experimental analyses for each test a variation was found, see Table 18. The FE-model showed almost for every comparison a larger bulging than the measured values.

A calculation was made to obtain the offset that the FE-model had to be calibrated with to consider the residual deformations. The differences of the total bulging in Test 1 between the experimental analyses and the FE-model were calculated, likewise the difference in Test 2 and Test 3. The total bulging of the experimental tests are shown in Table 9-11 and the total bulging of the FE-model for each tests are shown in Table 15-20.

Test 1	Offset [mm]	
IGU	Calliper	Laser
1	2.6	2.0
2	3.8	4.0
3	5.2	4.5
4		
5	3.7	3.3
Test 2	Offset [mm]	
IGU	Calliper	Laser
1		
2	3.7	2.8
3	3.9	3.6
4	3.4	
5	3.5	2.8
Test 3	Offset [mm]	
IGU	Calliper	Laser
1	3.4	3.1
2	4.6	4.3
3	5.9	5.5
4	2.5	3.1
5	3.7	3.6

Table 19. Difference between modelling analyses and experimental analyses, test by test.

As can be seen in Table 19, the offset was approximately 2-5 mm. The FE-model has to be added with this offset to give the same values as the experimental analyses.

6.2 Discussion about the comparison

As shown in Table 18 the FE model resulted in higher total bulging than the measured values, neglecting the residual deformations which occurred. Due to time constraints the model was not changed after the experimental analyses to fit better to the reality.

The residual bulging is shown as the offset in Table 19 which probably occurred due to some plastic deformations in the sealant or the spacer. However, the model was still used in a parameter study and was not changed with this offset. In future work this offset might be taken into consideration but need some further study.

7 Parameter Study

The main program was written as a Python script with preferred input data for IG units that were to be analysed. The 1D-FE model was also written as a Python script, it retrieved needed data from the main program and calculated the average temperatures in the cavities i.a. outside, inside temperatures and space distances. The main program received the temperature in the cavities and the bulging of the IGU was analysed in the FE model. The displacements and stresses in the glass panes were saved in a text file. The process is illustrated in Figure 18. From the obtained results a regression model was made that is described in Chapter 8.
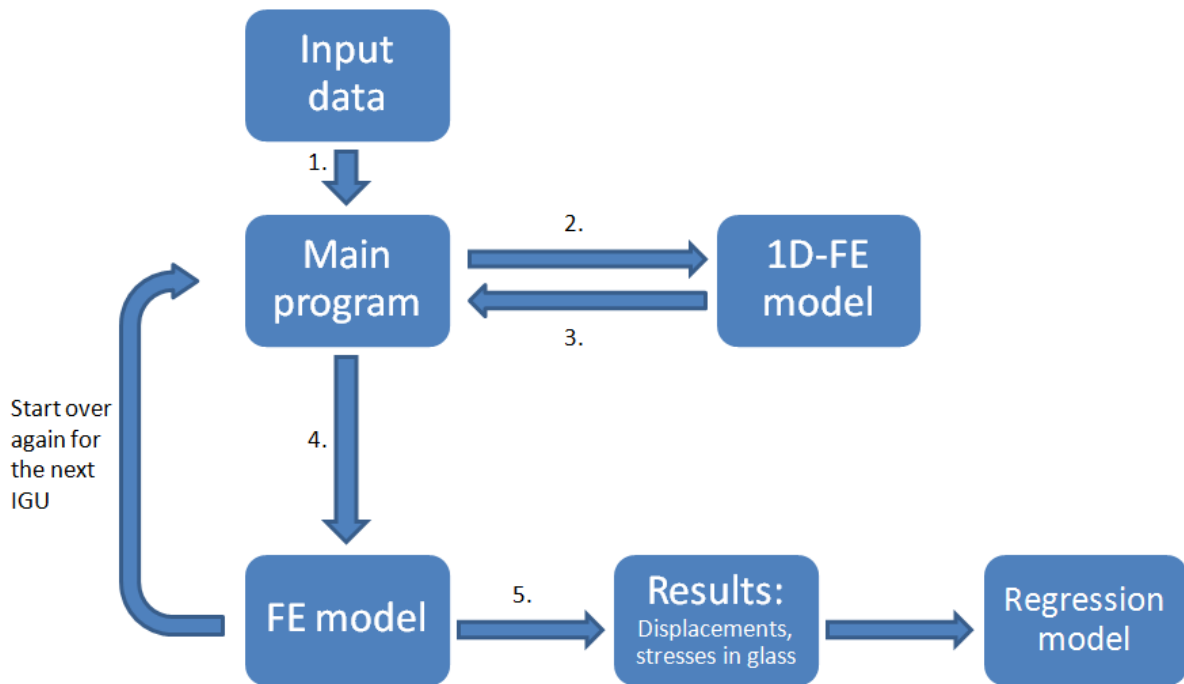

Figure 18. Illustration of the analyse procedure.

7.1 Material properties

The materials which were used are described in Chapter 2 and used in the parameter study are summarized in Table 20, 24 and 25.

Material	Young's modulus [MPa]	Poisson's ratio	Density [kg/m^3]	ε Annealed, low-E	λ [W/mK]	Optical properties
Glass	70 000	0.22	2500	0.837, 0.037	0.81	See Table 3,4 and 5

Table 20. Properties of glass.

To reduce the emissivity the glass could have a low-E coating. The optical properties i.e. the transmittance, the absorbance and the reflectance varies with the thickness and if the glass has low-E coating, see Table 3, 4 and 5. Some of the glass panes were coated in the parameter study.

The Young's modulus of the sealants and the spacer are shown in Table 21.

Material	Young's modulus [MPa]	Poisson's ratio
Butyl	2.13	0.2
Polysulfide	1.6	0.2
Spacer	$2900 \cdot h_{spacer}$	0.3

Table 21. Young's modulus and Poissn's ratio of the sealants and the spacer.

The Young's modulus of the spacer changes with the height of the spacer i.e. the space distance of the cavity.

Material	Gas type	Properties
Gas	Air, Argon, Krypton	See Table 6

Table 22. Properties of gas.

The thermal conductivity, specific heat capacity and the dynamic viscosity properties of the gases are varying with the temperature but the molecular weight was constant. When the cavities are filled with argon or krypton a gas content of 90% was assumed i.e. 10% was air.

7.2 Loads

The sealant in the IGU is exposed to various load types as described in Chapter 2.3. But the focus in this project was to determine the stresses and the displacements of the glass panes. Wind pressure and accidental load are two load types which will not be further investigated. Accidental loads on the IGU such as a ball hitting the glass pane or a child running in to the glass pane may occur, and the solution would be to have toughened or laminated the glass panes. The glass panes must also be of toughened glass if the glass panes' lower edges in a building are mounted lower than 0.6 m from the floor or the ground [7].

The wind pressure in Sweden is approximately 1 kPa [14]. This is relatively small compared to the variation in atmospheric pressure which is described further in this chapter. Therefore the wind load was neglected in this study.

The loads affecting the IGU that will be further investigated are the variation of temperature and atmospheric pressure. When the gas in the cavity has a lower pressure than it is outside of the cavity due to lower temperature of higher atmospheric pressure than the initial values an inwards bulging will occur. For the opposite load effects, the bulging of the glass panes will be outwards, see Figure 1.

7.2.1 Temperature load

The initial gas temperature in the IGU when manufactured was assumed to be same as was in the factory, approximately 20°C.

The temperature load will differ depending on the geographic location where the IGU is installed and at what season of the year it is. The average 3-hour temperature has been collected for the past 50 years from SMHI [19], with data from 1961 to 2011. A compilation of the temperature occurrences was made for five different cities; Kiruna, Luleå, Norrköping, Växjö and Malmö. These cities were chosen to get an overview of temperatures over Sweden.

Växjö was chosen since it is located near Lenhovda, the place for manufacturing the IG units used in this study. The temperature occurrences for Växjö and Luleå are shown in Figure 19.

7.2.2 Atmospheric pressure

When manufacturing the IGU the gas pressure was assumed to have the same pressure as the atmospheric pressure in the factory that day. The average atmospheric pressure which occurs the most in Växjö have been used as the initial value which was set to 99.5 kPa, see Figure 19. When the IGU is installed there may be a different ambient pressure than the pressure in the cavity. The difference in pressure will give a low pressure or an excess pressure in the cavity. A high pressure will give inwards bulging while a low pressure will give outwards bulging of the glass planes. The pressure was chosen to give a higher bulging in the study, both for inwards and outwards bulging.

As for the temperature, the atmospheric pressure has also been collected for five cities over a 50 year period.

The temperature and atmospheric pressure occurrence are shown in Figure 19 for the two cities mentioned previous. For data regarding other cities, see Appendix A
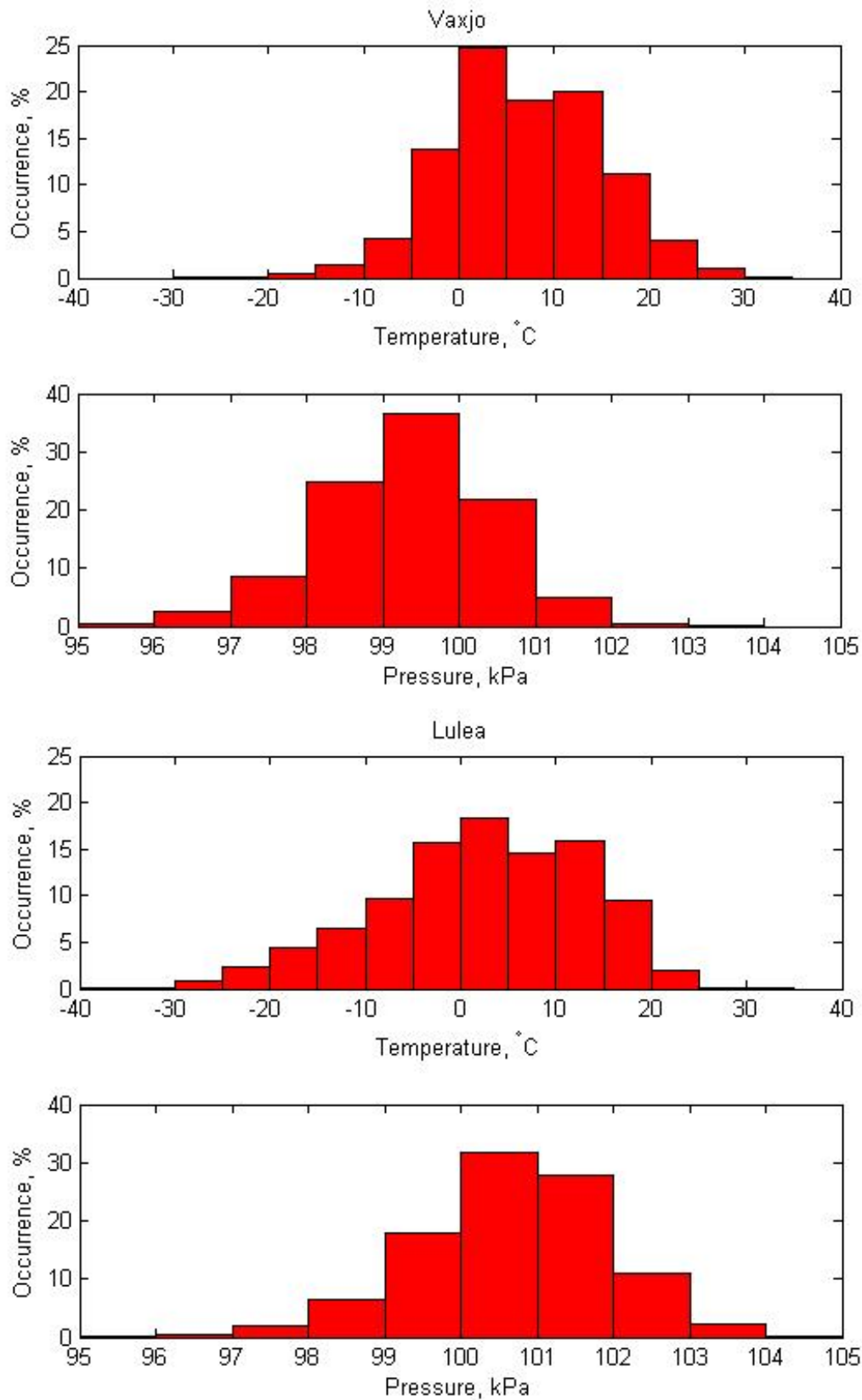
Figure 19. Temperature and pressure occurrence in Växjö and Luleå.

As shown in Figure 19 the atmospheric pressure in Växjö is generally a bit lower than the normal value of 101.3 kPa. In Luleå the pressure is normally higher than Växjö and quite low temperatures can occur which would give significant bulging.

From collected data the maximum and minimum temperatures each year was extracted and is shown in Figure 20 for Luleå. In this figure the probability that a certain temperature occurs in the city can be found. Maximum and minimum temperatures for other cities is presented in Appendix A
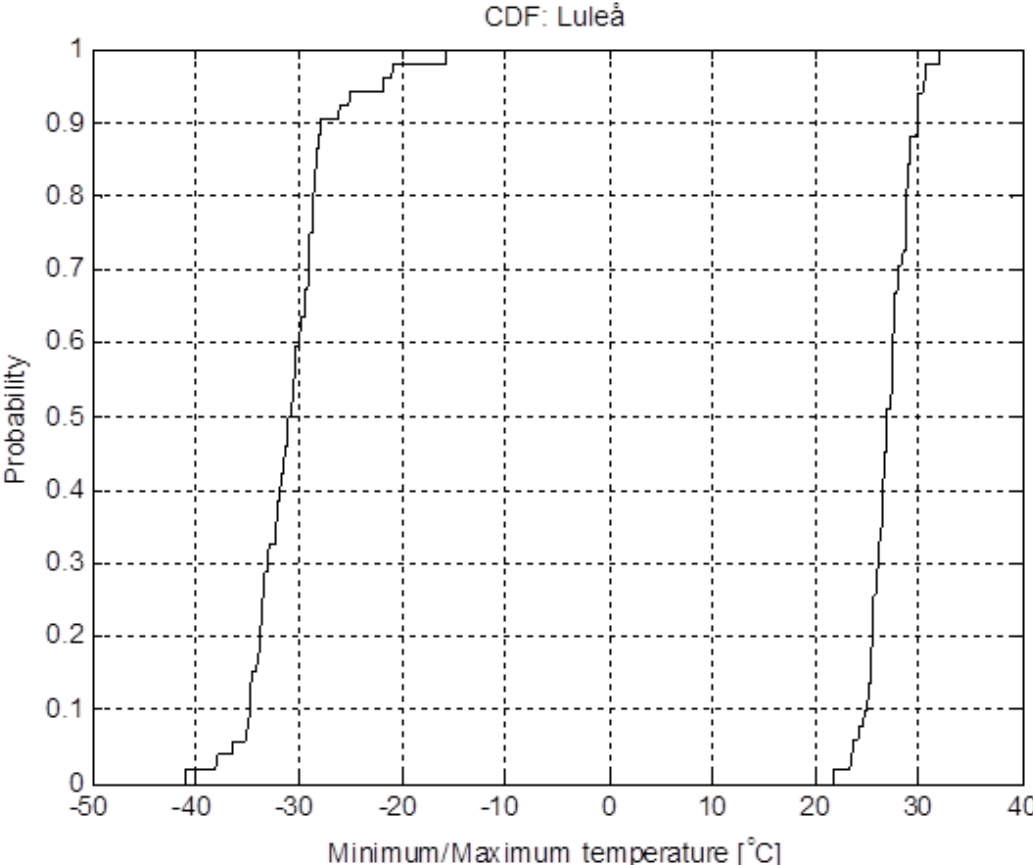
Figure 20. The probability of minimum and maximum yearly temperature occurance in Luleå.

47

7.3 Parameters

The parameters that were changed in the parameter study and how they were changed are presented below:

Parameter	Values	Comment
Width [m]	0,3-1,6	Both quadratic and rectangular dimensions were chosen.
Height/Width ratio	1-3	Most of the analyses were made with a height/width ratio lower than 1.5 but some were more elongated.
Glass thickness [mm]	1.8, 3.8, 5.8	Some varying combinations were made for the three glasses but the normal combination was 3.8 mm for all the glass panes.
Outer cavity [mm]	8-27	Different combinations of the outer and inner space distances were chosen.
Inner cavity [mm]	8-27	When an integrated blind was modeled the inner cavity had a distance of 22 mm.
Gas type	Air, Argon, Krypton	The same gas in both cavities.
Inner temperature [°C]	20 and 25	The inner temperature was kept constant to 20°C except when an integrated blind was placed in the inner cavity, an inner temperature of 25°C was chosen.
Outer temperature [°C]	-40 to 0 20 to 35	The outer temperature was varied between -40°C to 0°C during a cold day and 20°C to 35°C on a warm day.
Pressure [kPa]	0 to 7	The pressure difference between the initial pressure and the atmospheric pressure was varied between 0-7 kPa.
Solar radiation	$I_0 = 1090$ [W/m^2] $\alpha = 30°$	The effect of solar radiation was controlled which increased the temperature in the cavities in the 1D-FE model. The solar radiation was analysed when the outside and inside temperatures were 25°C.
Integrated blind	Absorbance=0.31 Reflectance=0.7 ε=0.8	The integrated blind was placed in the inner cavity and assumed to be closed when it was 25°C outside and inside and with the IGU exposed to solar radiation which increased the temperatures in the cavities.
Position and number of low-	Two low-E on surface 2 and 5	The low-E coatings were usually placed at surface 2 and 5, see Figure 7. But when an integrated blind

E coatings	One low-E on surface 2	were modeled in the 1D-FE model some analyses were made when it only was one low-E coating on surface 2.
Cold clear sky	Extra R value $\varepsilon=1$ T=-273.15°C	An extra R value was defined on the outside. Only theoretical value. The emissivity was assumed to be 1 and the temperature of the outer space was assumed to be -273.15°C.

Table 23. Parameters that were analysed are described.

If every combination of the parameters were analysed the total computing time would be very long. Therefore the focus was a winter day i.e. when the outdoor temperature is low and problems may occur where an integrated blind in the IGU may be clamped between the glass panes due to the bulging. 7 parameters that affect the bulging the most were varied, i.e. width, height/width ratio, outer cavity, inner cavity, outdoor temperature, atmospheric pressure and glass thicknesses. To get a good approximation the 7 parameters were varied with 5-6 steps each. One combination took around 1 minute, see Figure 17, if all combinations were analysed the total computing time would be approximately $5,5^7 \approx 152\,000\,\mathrm{min} \approx 100$ days. To reduce the computing time but still have 5-6 steps for each parameter, every 47th combination was analysed. The combinations were chosen as random as possible. The computing time was reduce to approximately 2 days and 3000 combinations of IG units were analysed, which were enough to get a good third-degree approximation. More about this approximation called regression model in Chapter 8.

7.4 Examples
Since many analyses were made, only some of the results will be presented here. These examples are a winter day, winter night with clear sky, summer evening and summer evening with blinds.

7.4.1 Winter day
In this example an IGU with an integrated blind is assumed to be installed in Luleå. Analyses were made to investigate how cold it could be outside for the blind to not get clamped i.e. when the displacement of the inner or the middle glass was 3.25 mm. The inner cavity with an initial distance of 22 mm, made for an integrated blind was chosen. The initial values of the temperature and pressure of the gas was taken from Växjö in Figure 19 and were set to 20°C and 99.5 kPa. It was assumed that the atmospheric pressure in Luleå was 102.5 kPa, 3 kPa higher than the initial value, see Figure 19. The distance of outer cavity was varied between 10-24 mm and the dimensions of the IGU varied between 0.8x0.8m^2 to 1.4x1.4m^2.

Analyses of the maximum principal stresses in the glass panes were also carried out for some IG units for the Luleå conditions. The atmospheric pressure was set to 103.5 kPa, 4 kPa higher than the initial value. The outside temperature was set to -30°C, see Figure 20 with a probability of approximately 7% to occur during a winter. The inner cavity was set to 22 mm while the outer cavity was varied between 10-24 mm and the in-plane dimensions were varied between 0.4x0.4m^2 to 0.8x0.8m^2.

The Luleå conditions cover many other places in Sweden for the winter load case since very low temperature can occur while the atmospheric pressure can be high.

7.4.2 Winter night with clear sky

For a case with a clear cold sky, the warmer IGU will emit energy to the colder sky. This will lead to a lower temperature in the outer glass with a higher risk for the glass to crack. The surface value of the outside temperature to give the same stresses as for a winter day will be calculated in this example.

The stresses in the glass were analysed for the Luleå conditions on a cold night having a high atmospheric pressure of 103.5 kPa.

7.4.3 Summer evening

In this example analyses of the maximum principal stresses in the glass panes were carried out for some IGU assumed to be placed in Växjö. During the evening when the sun is quite low and when it still is 25°C outside, the temperatures in the IGU can be high. The indoor temperature was set to 25°C and the incidence angle of the solar radiation was assumed to be 30°. The atmospheric pressure was varied and assumed to be 3 kPa or 1 kPa lower than the initial pressure in the cavities. The dimensions were varied between 0.4x0.4m^2 to 0.8x0.8m^2 and the outer cavity was varied between 10-24 mm.

To analyse the Växjö conditions for a summer evening covers many other places in Sweden since it may occur at most locations.

7.4.4 Summer evening with blind

To keep the solar radiation out during a summer evening the integrated blind could be lowered and closed. But the blind absorbs more energy and the temperatures in the IGU will increase and higher stresses in the glass panes may develop. In this example analyses were made with the same geometries, temperatures and solar radiation as for the summer evening but with the difference that an integrated blind was placed in the inner cavity. The pressure was 3 kPa lower than the initial pressure in the cavities. The effect of the location of the low-E coating was analysed to only have one low-E coating placed on surface 2, see Figure 7.

7.4.5 Overall analyses

Some overall analyses where when changing parameters such as glass thickness, gas content and the height/width ratio was varied.

An IGU with the distances 22 and 16 mm in the inner and the outer cavities respectively and with the dimensions 0.6x0.6m^2 were analysed when the gas type and glass thicknesses were changed. The outside and inside temperatures were set to -25°C and 20°C and the pressure was set to 3 kPa higher than the initial pressure in the cavities. The glass thicknesses 1.8, 3.8, and 5.8 mm were analysed with some different combinations in the three glass panes. The gas in the cavities were analysed with air, argon or krypton.

In the analyses where the height/width ratio was changed an IGU with the width of 1.2 m was used and only the displacements of the glass panes were determined. For analyses regarding the stresses smaller widths were chosen to 0.3, 0.4 and 0.6 m while the height was varied. The

same temperatures, pressure and distances of the cavities were chosen as in the analyses when varied the glass thicknesses and the gas type were varied. The glass thicknesses were set to 4, 4, 4 mm.

7.5 Example result

The results of the examples described above are presented below.

7.5.1 Winter day

The coldest outside temperature that can occur for an integrated blind to not get clamped in an IGU is presented in Figure 21. The pressure is 3 kPa higher than the initial value and the geometry varies.
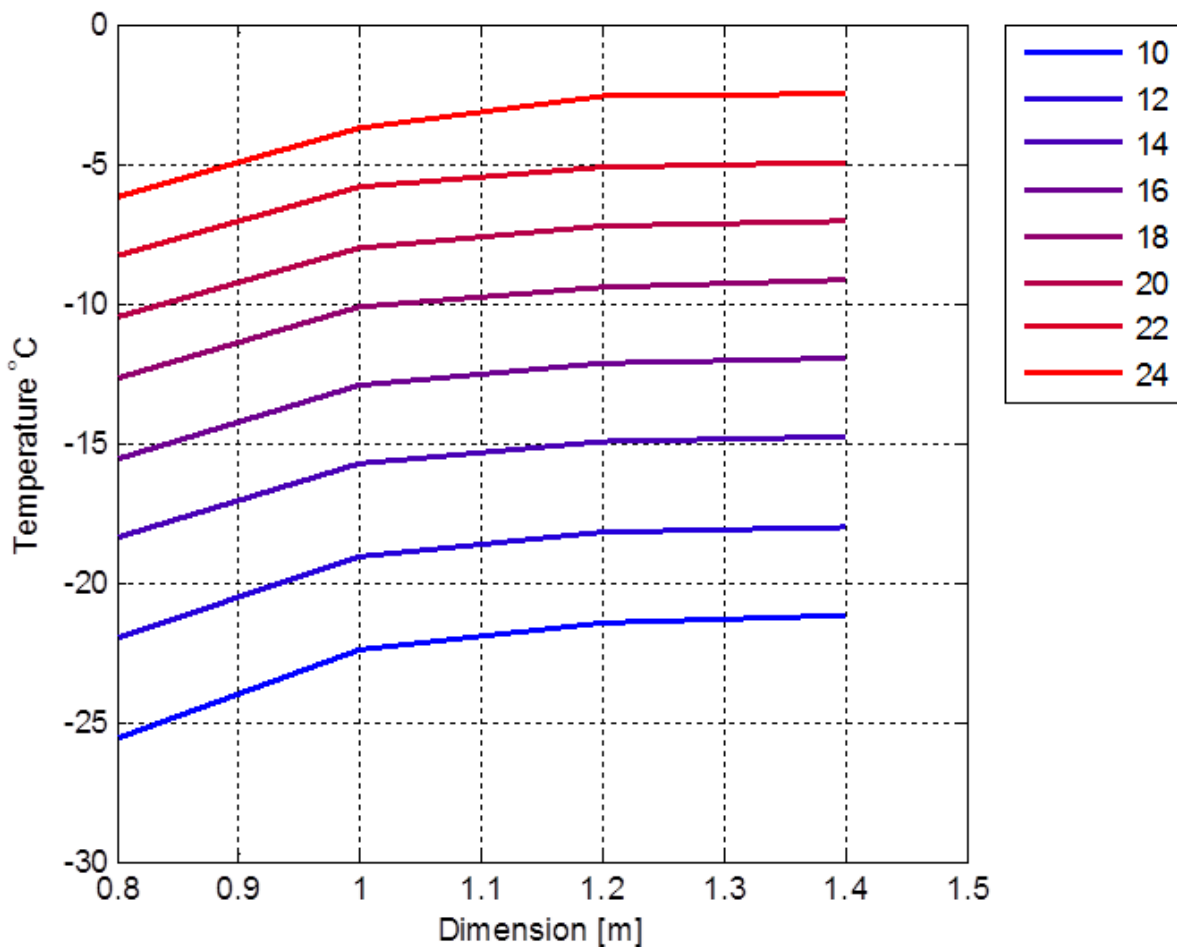
Figure 21. Minimum temperature for having an integrated blind for quadratic dimensions when varying the outer space.

As an example, a blind that is not allowed to be clamped at an outdoor temperature of -20°C only an IGU with an outer space distance of 10 mm could be chosen but the in-plane dimensions could be chosen freely.

The maximum principal stress, which occurred in the outer glass pane, for a pressure of 3 kPa higher than the initial value and for an outside temperature of -30°C is presented in Figure 22.
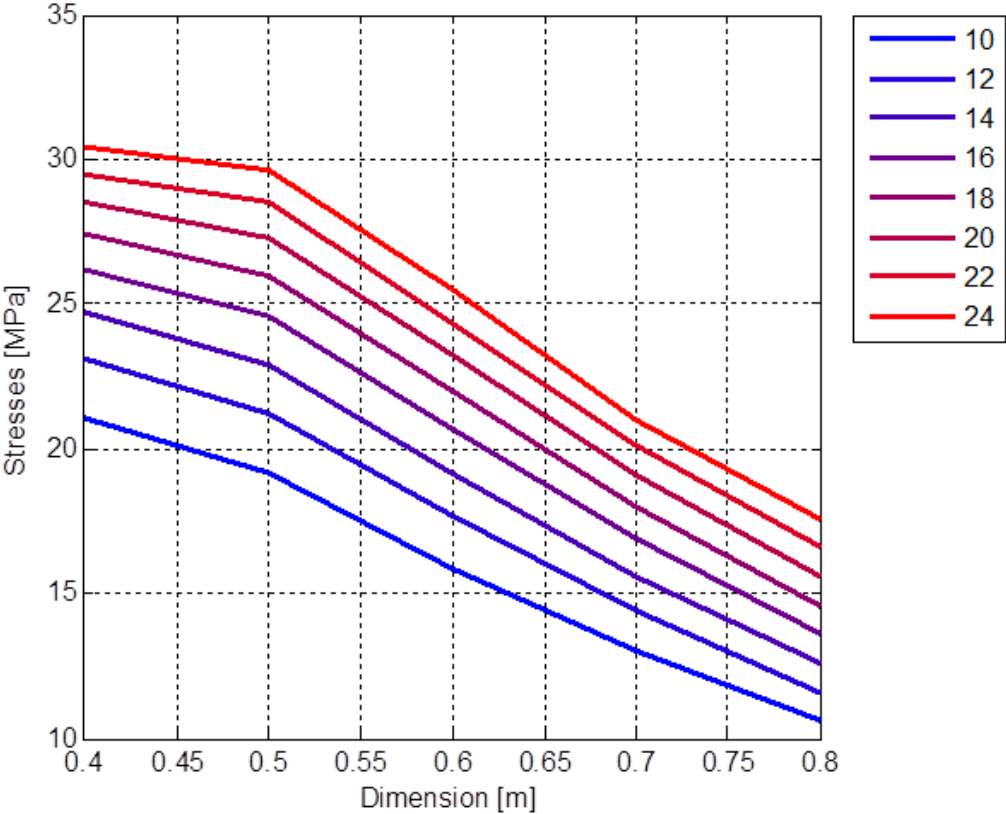

Figure 22. Stress in the outer glass on a winter day for quadratic dimensions when varying the outer space.

7.5.2 Winter night with clear sky
To obtain the same stress level on a winter night with clear sky as on a winter day the outdoor temperature could theoretically be 4-5°C higher. This is due to that the IGU emits energy to a colder sky.

7.5.3 Summer evening
The highest principle stress in the glass panes occurred when the outdoor and indoor temperatures were both 25°C. The analyses were made with an atmospheric pressure of 3 kPa and1 kPa lower than the initial pressure and the incidence angle of the solar radiation was 30°. The result is shown in Table 24.

Stress [MPa]	Pressure [kPa]	
Dimension [m^2]	- 3	- 1
0.3x0.3	15.2	12.5
0.4x0.4	**19.8**	**16.3**
0.5x0.5	**20.2**	**16.7**
0.6x0.6	**18.0**	14.9
0.7x0.7	15.2	12.6
0.8x0.8	12.5	10.4

Table 24. Stresses in the outer glass for a summer evening.

The not bold marked values are glass panes that do not have to be toughened. The tensile strength of glass was calculated to 15.48 MPa, see Chapter 3.5.

7.5.4 Summer evening with blind

When an integrated blind was lowered and closed, and when the number of low-E coatings were changed the highest tensile stress became as presented in Table 25.

Stress [MPa]	Low-E coating	
Dimension [m^2]	Surface 2,5	Surface 2
0.3x0.3	**34.4**	**26.7**
0.4x0.4	**40.8**	**32.9**
0.5x0.5	**38.7**	**32.0**
0.6x0.6	**33.3**	**27.8**
0.7x0.7	**27.8**	**23.2**
0.8x0.8	**23.0**	**19.2**
0.9x0.9	**19.0**	**15.9**
1.0x1.0	**16.0**	13.3

Table 25. Stresses in outer glass for a summer evening with an integrated blind.

The not bold marked values are glass panes that do not have to be toughened. The tensile strength of glass was calculated to 15.48 MPa.

7.5.5 Overall analyses

To see how different parameters effect on the displacement and principal stresses only one parameter changing at the time. In figure 23 the absolute displacement for a windows with different height/width ratio in-plane is changing. The width was kept constant to 1,2 m and the height varied.
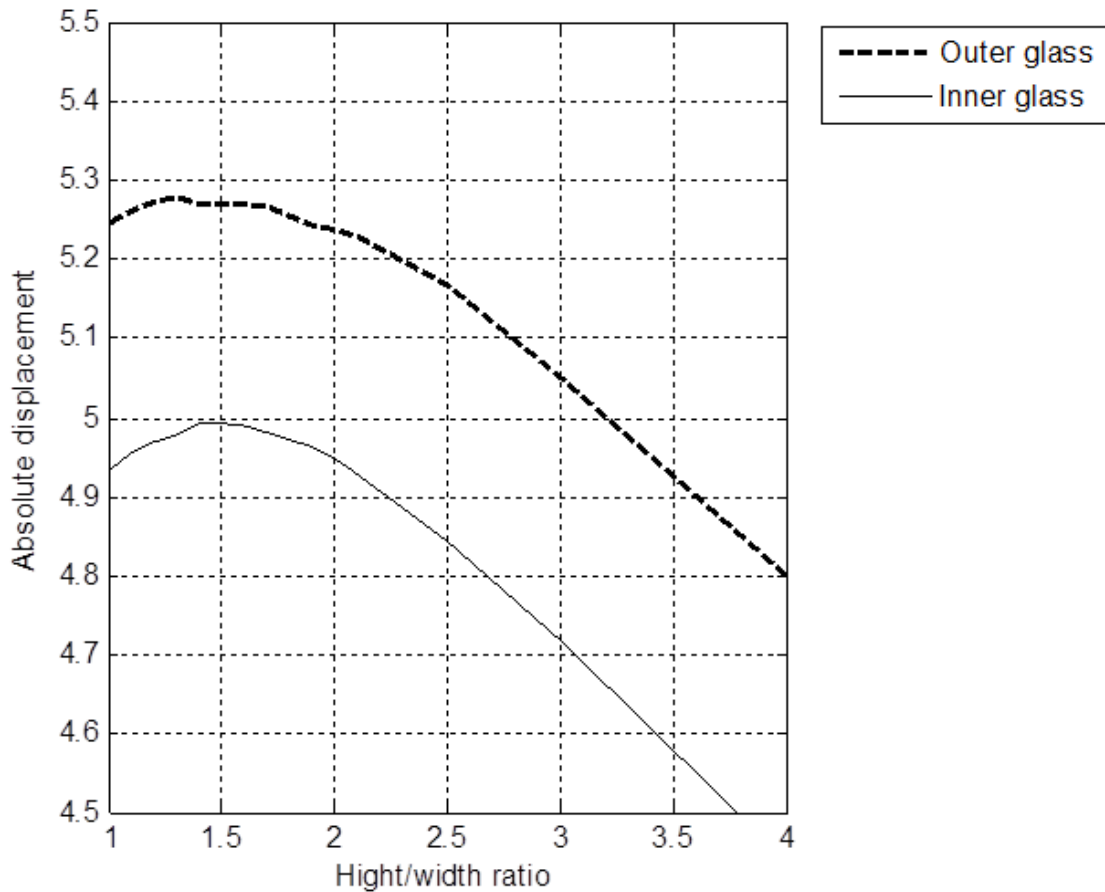

Figure 23. Displacement in inner and outer glass when changing the height/width radio.

The maximal principal stress in the outer glass pane is presented in Table 26 for a small width with varying height.

Stress [MPa]	Width [m]		
Height [m]	0,3	0,4	0,6
0,3	18,0		
0,4	23,2	20,6	
0,6	27,6	24,5	16,0
0,8	28,7	25,5	15,8
1,0	28,7	25,6	15,5
1,2	28,4	25,3	15,2
1,6	27,7	24,4	14,7
2,0	27,2	23,6	14,1

Table 26. Stresses in outer glass when varying the height and width.

The displacements and stresses for some different combinations of glass thicknesses in the three glass panes are presented in Table 27.

Glass thicknesses [mm]			Displacements [mm]			Stress [MPa]	
Outer	Middle	Inner	Outer	Middle	Inner	Outer	Inner
3.8	3.8	3.8	3.4	-0.7	-2.9	16.6	13.9
5.8	3.8	3.8	1.8	-1.7	-3.5	12.7	17.1
3.8	3.8	5.8	3.9	0.1	-1.5	19.1	10.2
5.8	1.8	5.8	2.1	-1.2	-2.0	14.5	13.9
5.8	3.8	5.8	2.2	-1.0	-1.9	15.4	13.2

Table 27. Analyses when changing the glass thickness.

The gas content in the cavities varied with the three gases air, argon and krypton. The stresses and the U-value are presented in Table 28.

Gas	Stress [MPa]	U [W/m^{2}K]
Air	19.0	1.03
Argon	18.9	0.82
Krypton	18.8	0.77

Table 28. Analyses when changing the gas in the cavity.

8 Regression Model

Multiple regression

The aim of a regression model is to find a function best suited for obtained data. A multiple regression investigates the relations between the parameters i.e. the parameters which were changed in the parameter study. If the system has more equations than solutions the system is overdetermined. The system can be written as: [33]

$$Ax = y \tag{8.1}$$

Where A is the different parameters matrix, x is unknown coefficients vector and y is the result vector.

A has the dimension mxn where m is the number of rows and n the number of columns. The x has to be a column-vector with the length n and y has to be a column-vector with the length m. If n and m is equal the system is determined i.e. if $\det(A) \neq 0$ the system has only one solution. If m is greater than n the system is overdetermined. The solution to find the x-vector for an overdetermined system with the least square method is as follows [33], where $\det(A^T A) \neq 0$:

$$Ax = y$$

$$A^T A x = A^T y$$

$$x = (A^T A)^{-1} A^T y \tag{8.2}$$

An example with two parameters which could be the height and the outdoor temperature with a polynomial of the second order are described below.

$$A = \begin{bmatrix} 1 & a_{11} & a_{12} & a_{11}a_{12} & a_{11}^2 & a_{12}^2 \\ 1 & a_{21} & a_{22} & a_{21}a_{22} & a_{21}^2 & a_{22}^2 \\ \vdots & \vdots & \vdots & \vdots & \vdots & \vdots \\ 1 & a_{n1} & a_{n2} & a_{n1}a_{n2} & a_{n1}^2 & a_{n2}^2 \end{bmatrix} \tag{8.3}$$

Where the second index in a_{ij} denotes which parameter the point belongs to. The first column only consists of ones which will give the first coefficient in x. Without this row the solution would go through origo. The second column is a vector of points of the first parameter. The third column is points of the second parameters. The fourth column is a product of the two factors of column two and three. The fifth and sixth is a quadratic term of the different parameters.

To calculate the coefficients in the x vector 5 to 6 arbitrarily points were chosen for every parameter in a specific interval. Since 7 parameters were varied a very large number of analyses would be necessary if all combinations were analysed. To reduce the number of analyses only the 47th combination was analysed. Approximately 3000 combinations of IG units were analysed which were enough to get a good function of the regression model. To

receive a good function it was important for the combinations and there varying parameters to be as random as possible. More combinations would give an even better approximation but these 3000 combinations were sufficient. A regression model was carried out for the summer and the winter loads. The best multiple regression was performed with a third-degree. The calculated coefficients in the function were compared with new points between the original points to verify that the regression model produce results with sufficient accuracy.

9 Discussion

In Figure 21 it is clearly shown that for large in-plane dimensions of IGU and a wider outer cavity, there is a higher risk for the integrated blind to get clamped. With larger dimensions, the glass panes get less stiff and a larger bulging occurs. An IGU with small in-plane dimensions will result in less bulging but higher stresses of the glass panes since the glass pane gets stiffer. In Figure 21 and Figure 22 it is shown that the stresses and the displacements increase with greater distance in the outer cavity. The reason for this is that a larger volume of the gas shrinks by lowering temperature which increases the bulging.

The stresses in a glass pane were bigger for the $0.5x0.5m^2$ than the $0.3x0.3m^2$, see Table 24. This is probably due to that for dimensions smaller than $0.5x0.5m^2$, a large amount of the load is carried by the spacers at the edges. For larger dimensions than $0.5x0.5m^2$ the stiffness of the glass panes decreases the principal stress decrease as well.

On a clear winter night the temperature in the IGU is lower than for a winter day, especially for the outer glass surface. Calculated values indicates that the outdoor temperature must be 4-5°C higher to result in the same stress levels as for a winter day, because of the radiation to the colder sky. This is a theoretical value, the assumed temperature of the outer space is probably a bit higher than -273.15°C and the assumed emissivity is probably a bit lower than 1.

When an IGU is exposed to solar radiation the temperatures in the cavities will increase. When a blind is integrated in the IGU it will increase the temperatures in the cavities since the blind absorbs a large amount of the solar energy. When the blind is lowered and closed the result will be an increase of the principal stresses in the glass panes, compare Table 24 and Table 25. The amount of and placement of the low-E coatings turned out to have a big influence on the principal stresses as shown in Table 25. By approximately estimate the maximal principal stress in advance, the glass panes exceeding the stress-limit can be toughened in the production state to avoid the glass panes to break in service.

In Figure 23 the height/width ratio affecting the displacements in the glass panes is shown with the constant width of 1,2 m. The worst ratio is found at 1.5. When a lower or higher ratio is chosen a smaller displacement occurs. For a smaller ratio, all of the edges have a larger influence to take the load. For a higher ratio, the IGU is more elongated and the smallest edges will have a lower influence to take the load. With increased height/width ratio the volume of the cavities increase, the cavities will work like springs and distribute the stresses through the system of the IGU. As shown in Table 26 the principal stresses for the widths 0.3 m and 0.4 m also have pikes when varying the height. It is concluded that there is a worst case ratio for the height and width for every specific IGU and need some further investigation.

The variations of the glass thicknesses were studied to see the affect on the displacements and stresses, see Table 27. If for example a thicker glass is chosen in the outer glass the principal stresses and the displacements decrease for that glass pane. However, the principal stresses and displacements increase for the inner glass. If an integrated blind would be installed a good

choice could be to increase the thickness of the inner glass pane, but that will result in high stresses in the outer glass and a control must be made if the glass needs to be toughened.

In the experimental analyses the gas content was a bit uncertain. The choice of gas will mainly affect the heat transfer through the IGU, see Table 28 but change of gas content did not result in a large varying of the stresses and the displacements.

10 Conclusion and further work

The objective of the study was to analyse the bulging of IG units for varying parameters such as the geometry and the magnitude of the loads. The primary goal is to determine the possibility of having an integrated blind in an IGU and to predict when the stresses become too high and the glass must be toughened.

The 1D-FE model gave a lower average temperatures in the cavities compared to the experimental analyses. The temperatures in the cavities were increased in the experimental analyses due to the effect of the bulging which changed the heat transfer through the IGU. With a small variation of the temperatures in the cavities a conclusion was that the 1D-FE model can be used to give a good approximation of the temperatures. A suggestion of further work is to find a way to take the bulging into consideration in the 1D-FE model.

The FE-model was compared with the experimental analyses and the model showed a bit higher bulging, if the residual deformations were neglected. The residual deformations in the IG units turned out to be quite big and some further study has to be done in this subject. No changes were made in the FE-model after knowledge about the residual deformations, the model was still used in the parameter study to give the bulging of the glass panes.

The regression model was carried out to fit a function for analysed data from the parameter study. The regression model is used to easy obtain the displacements and stresses in the glass panes varying the parameters as the user wants. The regression model is therefore a model that can give a good perception of the bulging so that blinds can be integrated and glass be toughened if needed. If the bulging sometimes becomes so big that the integrated blind gets clamped it will not lead to failure of the IGU, it will just result in that the blind can't be raised which there must be tolerance for.

The affect of solar radiation in the IGU was only considered in the FE model, some experimental analyses of this phenomenon can be made in a future work to get more knowledge about this.

11 References

[1] Burström P.G., *Byggnadsmaterial*, 2001, Lund, Studentlitteraturer.

[2] Glass for Europe. *Main types of glass,* http://www.glassforeurope.com/en/products/main-types-of-glass.php, visited 2014-04-01.

[3] Carlson P.-O., *Glas - Möjligheternas Byggmaterial,*1992, Stockholm, Statens råd för byggnadsforskning.

[4] Van Den Bergh S. et al., *Window spacer and edge seals in insulating glass units: A state-of-the-art review and future perspectives,* 2012, Elsevier B.V.

[5] Wolf A.T., *Studies into the life-expectancy of insulating glass units,* 1998, France, RILEM Publications SARL.

[6] Le Bourhis E., *Glass – Mechanics and Technology*, 2008, Weinheim, WILEY-VCH Verlag GmbH & Co.

[7] Boverkets byggregler, *BBR 20-8:353,* 2013.

[8] European standard, *Glass in building – Determination of the load resistance of glass panes by calculation and testing,* 2013, Technical Committee CEN/TC 129.

[9] European standard - EN 572-2, *Glass in building – Basic soda lime silicate glass products- Part 2: Float glass,* 2012, Technical Committee CEN/TC 129.

[10] Sandin K., *Praktiskt byggnadsfysik*, 2010, Lund, KFS.

[11] Pilkington, *Glasfakta*, 2012, NSG Group.

[12] Ethiopian standard – ES ISO 15099, *Thermal performance of windows, doors and shading devices -Detailed calculations,* 2012, Ethiopian Standards Agency ESA.

[13] Jelle B.P., *Solar radiation glazing factors for window panes, glass structures and electrochromic windows in buildings-Measurement and calculation*, 2013, Elsevier B.V.

[14] Isaksson T. & Mårtensson A., *Byggkonstruktion – Regel- och formelsamling*, 2010, Lund, Studentlitteraturer.

[15] Ottosen N.S. & Petersson H., *Introduction to the Finite Element Method*, 1992, Lund, Prentice Hall.

[16] Guardian Europe S.à r.l. Dudelang, *Glass Time-Technical manual*, 2012, Luxembourg, Guardian|mkt.

[17] Larsson U. et.al., *Thermal analysis of super insulated windows (numerical and experimental investigations)*, 1999, Elsevier Science S.A.

[18] Hautekeer J.-P. et al*., Key factors governing technologies on the growing China Insulating Glass Market*, Dow Corning.

[19] SMHI, http://www.smhi.se, visited 2014-01-30 to 2014-06-03.

[20] Persson K., Unpublished data, The Division of structural Mechanics, Lund University, 2013.

[21] Backman H.E. *The insulating glass unit in europe - materials and experiences PDF,* 1998, Sweden, RILEM Publications SARL.

[22] Nationalencyklopedin, *solarkonstanten,* http://www.ne.se/lang/solarkonstanten, visited 2014-05-30.

[23] Pellini ScreenLine, *Venetian blinds SL20M, SL22M,* http://pellini.screenline.dk/brochurer/, visited 2014-06-04.

[24] Pellini ScreenLine, *Technical Catalogue,* http://pellini.screenline.dk/brochurer/, visited 2014-06-04.

[25] MatWeb, *Butyl Rubber,* http://www.matweb.com/search/DataSheet.aspx?MatGUID=754a0c3d7c194965a0b369792855bfe4 , visited 2014-06-03.

[26] Pentronic, *Termoelement teori,* http://www.pentronic.se/start/temperaturgivare/teori-om-givare/teori-om-termoelement.aspx , visited 2014-05-05.

[27] Björk L.-E. et.al., *Formler och tabeller,* 1998, Stockholm, Bokförlaget Natur och Kultur.

[28] Abaqus 6.12 SIMULIA, *Abaqus/CAE User's Manual - Interacting with Abaqus/CAE,* http://abaqus.me.chalmers.se/v6.12/ , visited 2014-06-26

[29] Abaqus 6.12 SIMULIA, *Abaqus Analysis User's Manual - Fluid cavity definition,* http://abaqus.me.chalmers.se/v6.12/ , visited 2014-06-26

[30] Abaqus 6.12 SIMULIA, *Abaqus Analysis User's Manual - Analysis Procedures,Solution, and Control-Static stress analysis-Nonlinear static analysis,* http://abaqus.me.chalmers.se/v6.12/ , visited 2014-06-26

[31] Python, *The Python Wiki,* https://wiki.python.org/moin/FrontPage , visited 2014-06-26

Verbal source:

[32] Karlsson A., Technical Advisory Manager Fire Protection Glass, Pilkington, 2014-04-11.

[33] Lübeck J., Excerpts from lecture notes in S*tatistikteori Linjär regression och stokastiska vektorer*, 2008, Matematisk statistik FMS012 LTH, 2014-07-07.

12 Appendix A

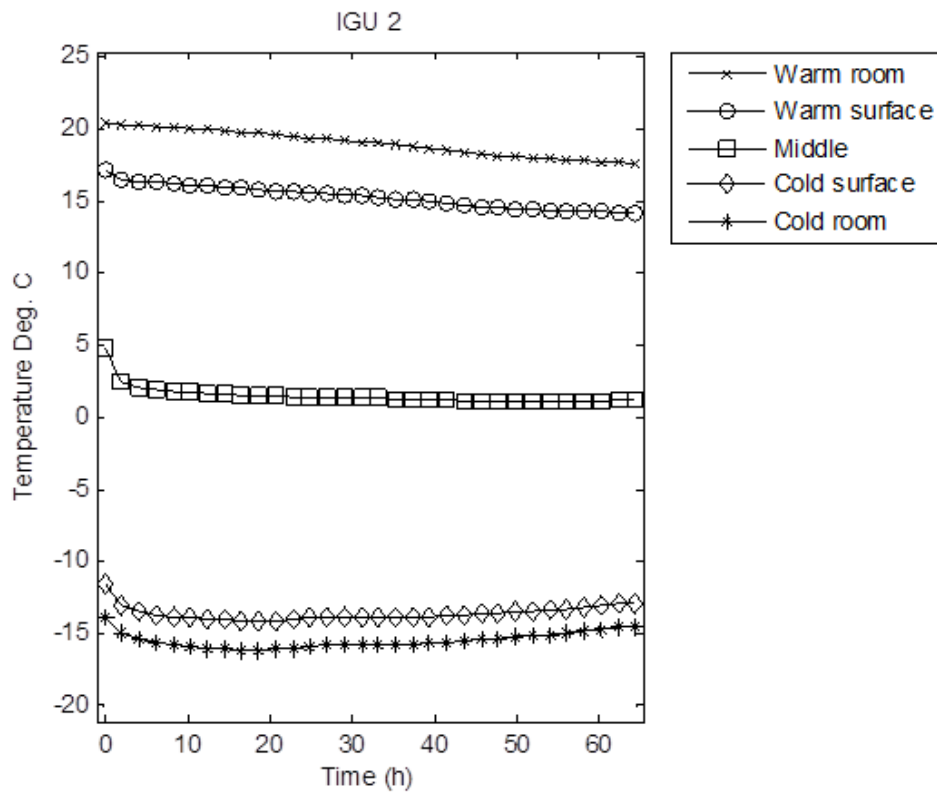## 12.1 Temperature distribution through tested IG units

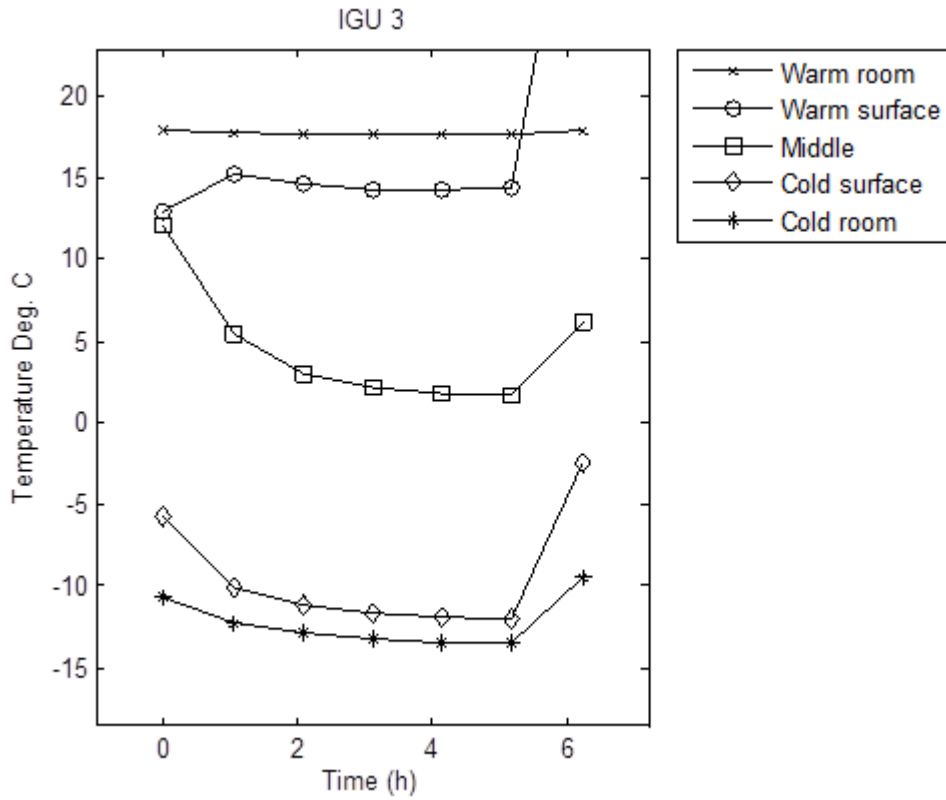**Figure 24. Temperature distribution through IGU 2.**

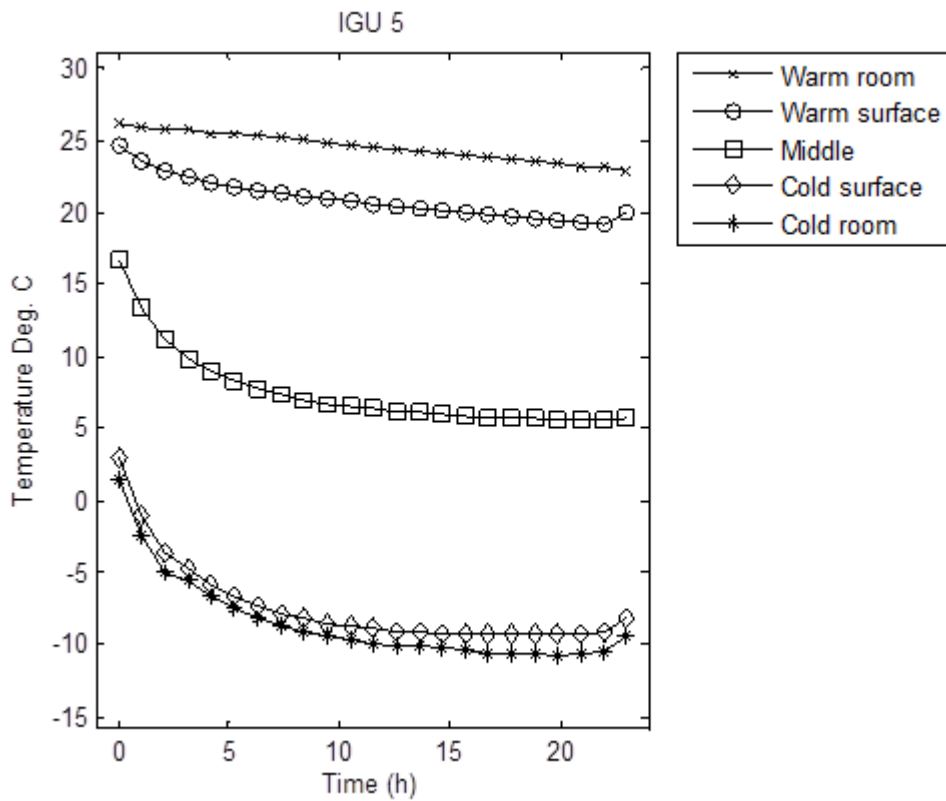**Figure 25. Temperature distribution through IGU 3.**

Figure 26. Temperature distribution through IGU 5.

12.2 Calibration factors and standard deviation of tests

The thermocouple wires were calibrated to the temperature in the cold room that was -10.15°C.

IGU	2	3	5	Wire W	Wire C
Logged temperature [°C]	-10.4	-9.77	-9.91	-10.05	-10.09
Calibration factor [°C]	0.25	-0.38	-0.24	-0.10	-0.06
After calibration [°C]	-10.15	-10.15	-10.15	-10.15	-10.15

Table 29. Calibration for the thermocouple wires.

Wire W and Wire C in was the thermocouple wires used on every IGU in the warm respectively the cold room. And the others, number 3,4 and 6 represent the thermocouple wire that where attached at the mid glass.

12.3 Standard deviations

Test 1	Standard deviation [mm]	
IGU	Calliper	Laser
1	0.3	0.5
2	0.1	0.4
3	0.2	0.4
4		
5	0.1	0.4

Table 30. Standard deviation Test 1.

Test 2	Standard deviation [mm]	
IGU	Calliper	Laser
1		
2	0.1	0.3
3	0.1	0.3
4	0.1	
5	0.2	0.2

Table 31. Standard deviation Test 2.

Test 3	Standard deviation [mm]	
IGU	Calliper	Laser
1	0.1	0.1
2	0.1	0.0
3	0.2	0.1
4	0.1	0.2
5	0.1	0.1

Table 32. Standard deviation Test 3.

13 Appendix B

13.1 Temperature and pressure occurence

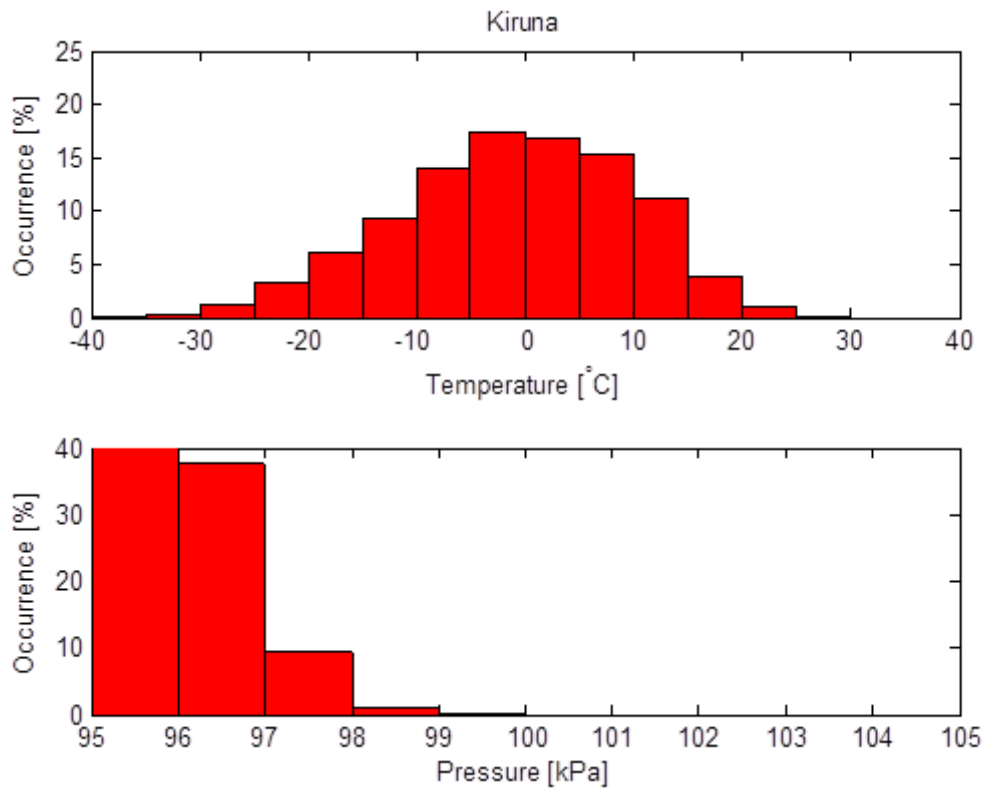Temperature and atmospheric pressure occurrence in Kiruna, Norrköping and Malmö.

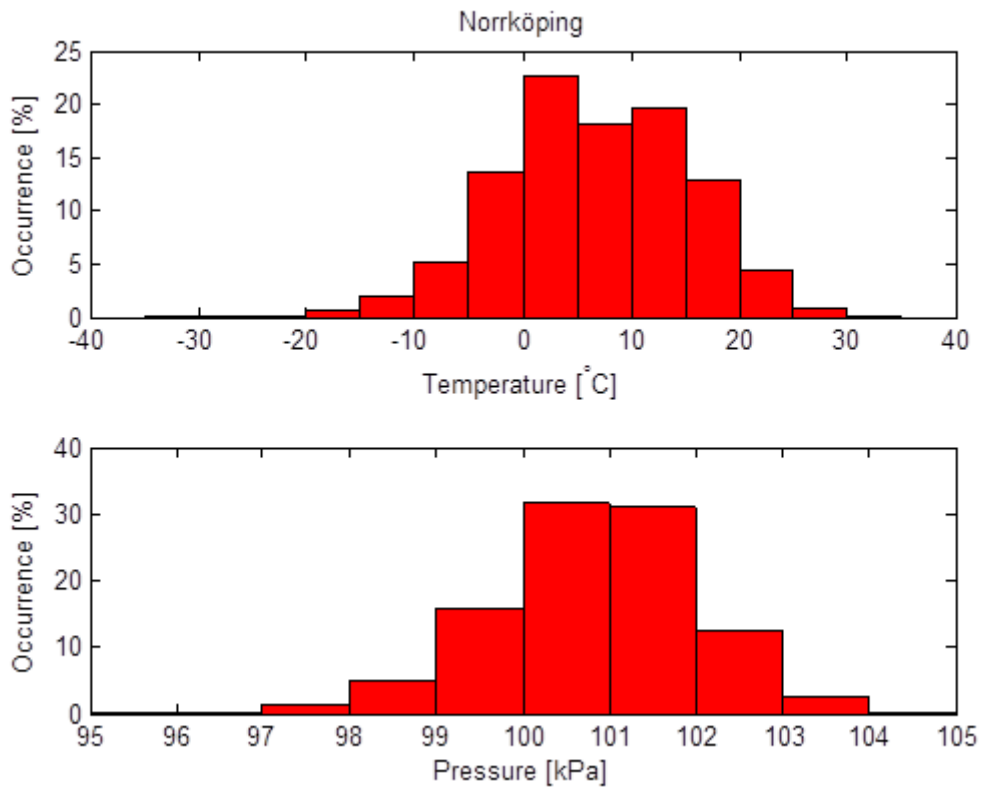**Figure 27. Temperature and pressure occurrence in Kiruna.**

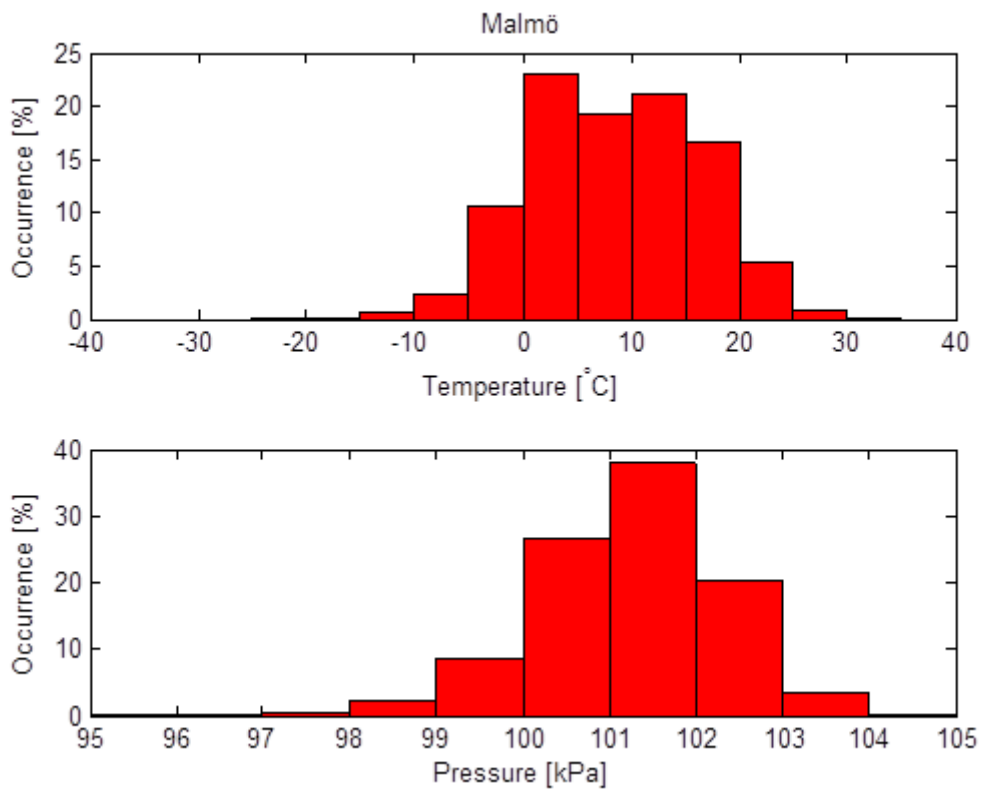**Figure 28. Temperature and pressure occurrence in Norrköping.**

Figure 29. Temperature and pressure occurrence in Malmö.

70

13.2 Minimum and maximum temperature

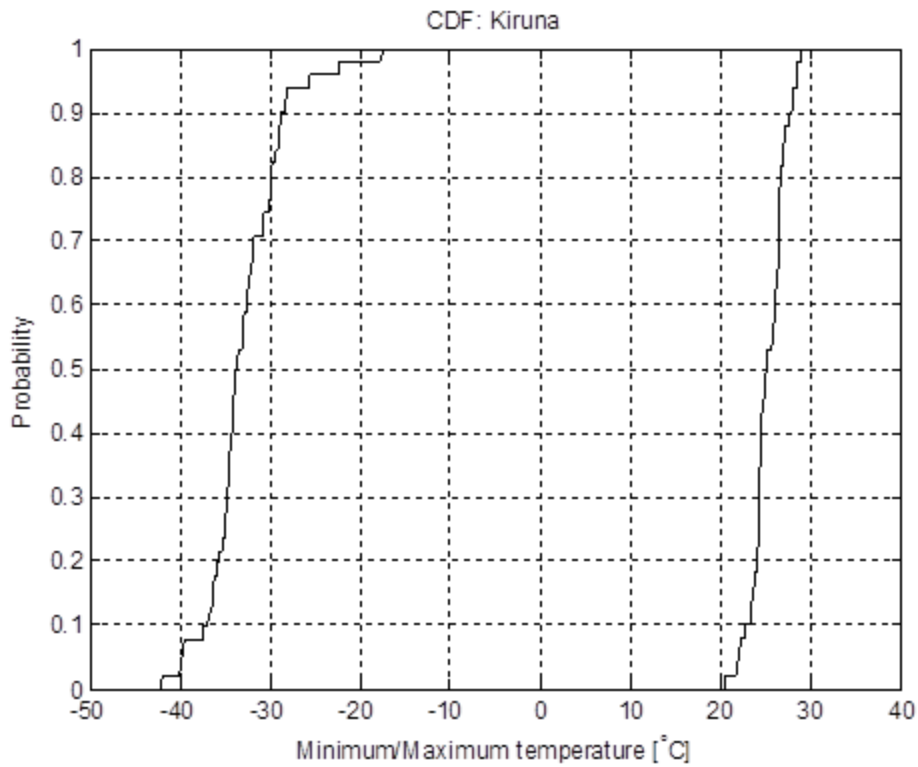Minimum and maximum temperature for Kiruna, Norrköping, Malmö and Växjö.

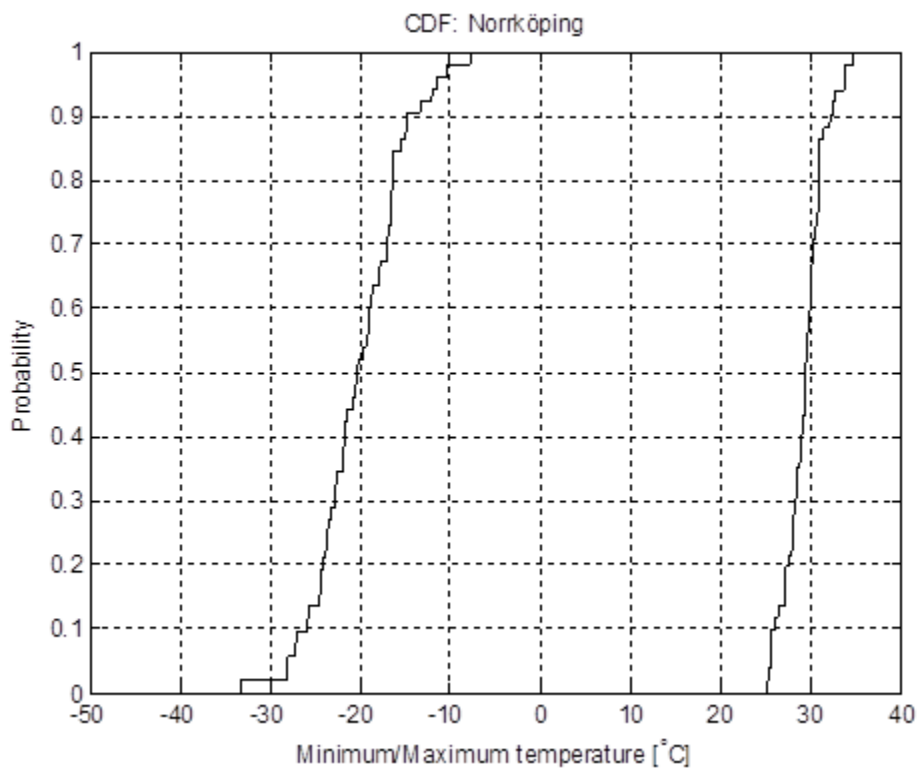**Figure 30. Probability of minimum and maximum temperatures in Kiruna.**

Figure 31. Probability of minimum and maximum temperatures in Norrköping.
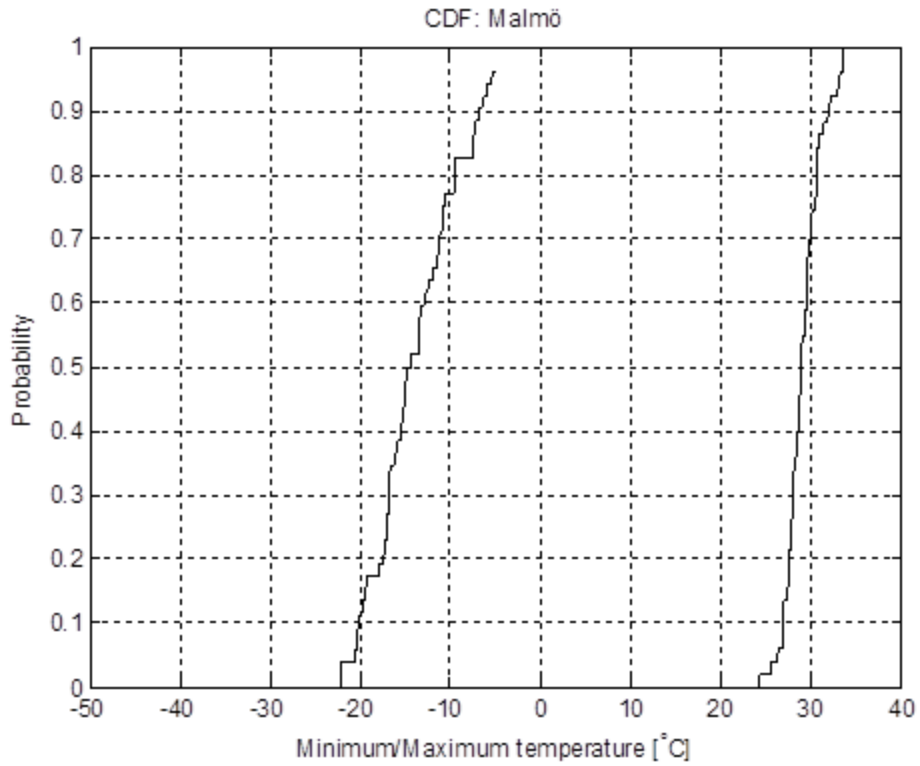
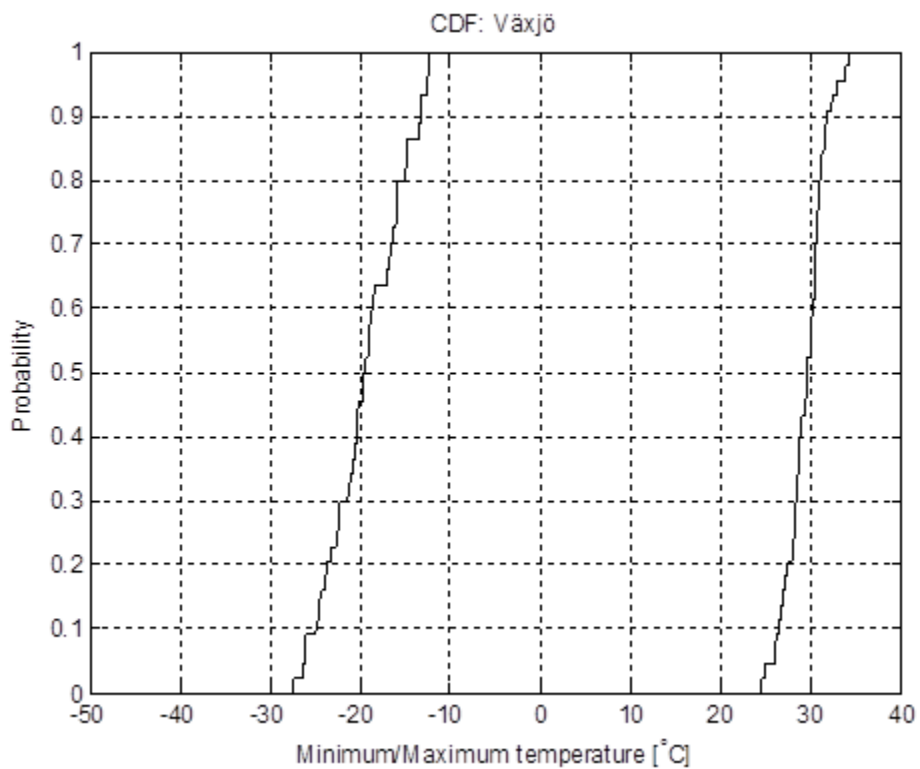**Figure 32. Probability of minimum and maximum temperatures in Malmö**

Figure 33. Probability of minimum and maximum temperatures in Växjö.